

ARTICLE



In individuals with Williams syndrome, dysregulation of methylation in non-coding regions of neuronal and oligodendrocyte DNA is associated with pathology and cortical development

Sari Schokoroy Trangle¹, Tali Rosenberg², Hadar Parnas², Gilad Levy³, Ela Bar^{1,4}, Asaf Marco^{2,5} and Boaz Barak^{1,3,5}

© The Author(s), under exclusive licence to Springer Nature Limited 2022

Williams syndrome (WS) is a neurodevelopmental disorder caused by a heterozygous micro-deletion in the WS critical region (WSCR) and is characterized by hyper-sociability and neurocognitive abnormalities. Nonetheless, whether and to what extent WSCR deletion leads to epigenetic modifications in the brain and induces pathological outcomes remains largely unknown. By examining DNA methylation in frontal cortex, we revealed genome-wide disruption in the methylome of individuals with WS, as compared to typically developed (TD) controls. Surprisingly, differentially methylated sites were predominantly annotated as introns and intergenic loci and were found to be highly enriched around binding sites for transcription factors that regulate neuronal development, plasticity and cognition. Moreover, by utilizing enhancer–promoter interactome data, we confirmed that most of these loci function as active enhancers in the human brain or as target genes of transcriptional networks associated with myelination, oligodendrocyte (OL) differentiation, cognition and social behavior. Cell type–specific methylation analysis revealed aberrant patterns in the methylation of active enhancers in neurons and OLs, and important neuron–glia interactions that might be impaired in individuals with WS. Finally, comparison of methylation profiles from blood samples of individuals with WS and healthy controls, along with other data collected in this study, identified putative targets of endophenotypes associated with WS, which can be used to define brain-risk loci for WS outside the WSCR locus, as well as for other associated pathologies. In conclusion, our study illuminates the brain methylome landscape of individuals with WS and sheds light on how these aberrations might be involved in social behavior and physiological abnormalities. By extension, these results may lead to better diagnostics and more refined therapeutic targets for WS.

Molecular Psychiatry (2023) 28:1112–1127; <https://doi.org/10.1038/s41380-022-01921-z>

INTRODUCTION

Williams syndrome (WS), also known as Williams-Beuren syndrome, is a rare genetic multi-systemic neurodevelopmental disorder caused by a pathological micro-deletion of 26–28 genes in the 7q11.23 region, also referred to as the WS critical region (WSCR) [1–3]. WS is characterized by social abnormalities, such as hyper-sociability, striking social fearlessness, distinct over-friendliness, and excessive empathy, along with poor social judgment ability [1, 4]. WS is also associated with distinctive facial features [5], cardiovascular abnormalities [6–8], endocrine imbalances [9, 10], severe visuospatial construction weakness [11–13] and intellectual disability [13–17]. The WSCR can undergo deletion, duplication, or inversion, with such aberrations having been associated with other disorders, such as autism [18, 19] and schizophrenia [19, 20]. Consistent with these phenotypes, previous studies revealed genome-wide transcriptional disruption in

various cell types and organs of individuals with WS [21–23]. Specifically, we previously showed reduction in myelin-related gene transcript levels, OL numbers, neuronal myelination [21] and white matter properties [24, 25] in individuals with WS, as compared to TD controls.

Although the molecular basis for the neurological phenotypes seen in WS has been intensively studied, the potential effect of WSCR deletion on epigenetic modifications remains poorly understood. To date, WS has been largely studied as a monogenic disease using mouse models in which the roles of individual genes were considered. While this approach is important for our understanding of each of these genes, multigenic mechanisms that modulate relevant gene expression and the subsequent effects on brain development are still largely unknown. Such multigenic effects could be regulated by epigenetic modifications which affect transcription without altering the underlying DNA

¹The School of Psychological Sciences, Faculty of Social Sciences, Tel Aviv University, Tel Aviv 6997801, Israel. ²Neuro-Epigenetics Laboratory, Faculty of Agriculture, Food and Environment, The Hebrew University of Jerusalem, Rehovot 7610001, Israel. ³Sagol School of Neuroscience, Tel Aviv University, Tel Aviv 6997801, Israel. ⁴The School of Neurobiology, Biochemistry & Biophysics, Faculty of Life Sciences, Tel Aviv University, Tel Aviv 6997801, Israel. ⁵These authors contributed equally: Asaf Marco, Boaz Barak. email: asaf.marco@mail.huji.ac.il; boazba@tauex.tau.ac.il

Received: 17 April 2022 Revised: 3 December 2022 Accepted: 12 December 2022
Published online: 28 December 2022

sequences. Such modifications could involve several processes, including DNA methylation, mRNA degradation via non-coding RNAs, and/or post-translational modifications of histones, DNA-associated chromosomal proteins [26, 27].

Although reversible, epigenetic changes are typically stable, presenting patterns that vary across cell types and throughout development [28]. It is now evident that errors in the epigenetic code, such as modifying the wrong gene or failure to add an epigenetic modification, can lead to abnormal gene activity, and thus could contribute to alterations in phenotype or to pathologies [29]. Interestingly, deletions of several genes in the WSCR locus were linked to epigenetic regulation [22, 23]. For example, *WBSCR22*, *BAZ1B*, and *BCL7B*, corresponding to WSCR genes, encode proteins involved in chromatin remodeling [30–33], while the product of *NSUN5* has been shown to act as an RNA methyltransferase [34]. Moreover, two additional WSCR genes, *GTF2I* and *GTF2IRD1*, encode proteins that have been shown to functionally interact with several regulatory complexes [35–39], chromatin and DNA modifiers [40, 41]. These include histone deacetylases (HDAC1-3) [42], lysine-specific demethylase 1 (LSD1), components of the repressive poly-comb complex [43, 44], and DNA-methyltransferase 3-like protein (DNMT3L) [45].

DNA methylation is one of the better-known epigenetic modifications and has been widely studied in the context of numerous biological and brain functions, including embryonic development [46–49], cell differentiation [50–52], neurodevelopment [53–55], myelination [50, 52, 56–60], neurogenesis and cell identity [46, 47, 61, 62]. Methylation of mammalian genomes occurs predominantly at cytosines adjacent to guanines ('CpG' sites) [61, 63]. As a result, the accessibility of the transcriptional machinery to a particular gene or given regulatory element (RE) may be altered. While *de novo* DNA methylation is predominantly regulated by DNA methyltransferase (DNMT) family members, active de-methylation is regulated by members of the ten-eleven translocase (TET) family of enzymes. Aberrant DNA methylation has been implicated in many neuropsychiatric disorders, including autism spectrum disorder (ASD) [64] and schizophrenia [65]. Previous work by Strong *et al.* examined DNA methylation patterns from blood samples taken from children with WS, 7q11.23 duplication syndrome (Dup7) and age-matched TD controls [22]. Their data revealed significant genome-wide differences in DNA methylation patterns across the WS and Dup7 groups, when compared to controls [22]. Specifically, these authors found enrichment of DNA methylation near transcription factor (TF)-binding sites, such as in *EGR1* and *EGR2*, genes associated with neuronal plasticity [66] and myelination [67], and in *FOXP1* and *FOXP2*, associated with developmental speech disorders [68]. The authors also showed that differentially methylated region (DMR) in individuals with WS are augmented with CCCTC-binding factor (CTCF)-binding sites, one of the major structural proteins that forms a physical bridge linking distinct DNA elements and plays a major role in spatial genome organization [69]. Follow-up research by Kimura *et al.* examined the global methylation status of blood samples from individuals with WS and TD controls [23]. In this study, individuals with WS exhibited significantly higher methylation levels than controls on several genes, including the *ANKRD30B* (ankyrin repeat domain-containing protein 30B) gene, previously linked to Alzheimer's disease [2, 70]. At the same time, hyper-methylation and lower levels of *ANKRD30B* transcription were found in brain samples of individuals with WS, relative to TD controls [23].

While these studies underscore the importance of DNA methylation for transcription, the precise effects of such methylation on the human brain and its relation to WS pathology remain largely unknown. As such, epigenetic studies can open new research directions focused on genes outside the WSCR and previously not considered to affect WS pathology and, hence, not previously addressed in the context of WS, so as to illuminate

novel mechanisms or pathways associated with this condition. Accordingly, in the present study, we considered Brodmann area 9 (BA9) sections from frontal cortex derived from individuals with WS and TD controls. Specifically, these samples were examined for whole genome methylation alteration.

Our data revealed genome-wide disruption of the methylome in individuals with WS, as compared to TD controls, as well as transcriptional networks and biological processes that might be altered by aberrant methylation. The affected pathways include genes highly associated with myelination and OL precursor cell (OPCs) differentiation, such as *GAD1*, *GPR17*, *ID4* [71, 72], *LINGO3* and *LINGO1* [73–75]. Finally, by correlating methylation profiles from blood samples and our data derived from brain samples, we identified putative targets that can be used to identify brain-risk loci for WS (outside the WSCR locus) and other associated pathologies.

Together, our study illuminates the epigenetic landscape of individuals with WS and helps to shed light on how epigenetic aberrations might be involved in social behavior and physiological abnormalities. By extension, these results will provide a better understanding of potential diagnostic and therapeutic targets.

RESULTS

7q11.23 deletion promotes genome-wide aberrations in the human frontal cortex DNA methylation landscape

To better understand the potential impact of the 7q11.23 deletion on the brain epigenome, we addressed DNA methylation (Fig. 1a) in BA9 in frontal cortex sections taken from three individuals with WS and five matching controls (for information on these subjects, see Supplementary Table 1). Reduced representation bisulfite followed by sequencing (RRBS) libraries were prepared from these brain tissues. Consistent with previous reports [22, 23], 1,862,636 single CpG sites across all samples passed quality control. These were subsequently subjected to paired (TD vs. WS) differentially methylated individual CpG site analysis, using the *edgeR* pipeline [76] with Benjamini-Hochberg multiple testing correction to control for the false discovery rate (FDR). Since sex and age are known factors for variation in DNA methylation, we included them as covariates in our differential analysis (see methods). Importantly, we performed another paired analysis, comparing either males to females (M vs. F, regardless of pathology) or younger vs. older (below and above the age median, respectively). Our data revealed genome-wide disruption in the methylome of individuals with WS, where 110 hyper-methylated sites (Hyper-DMSs) and 222 hypomethylated sites (Hypo-DMSs) were identified, as compared to the extent of methylation at the same sites in TD controls (Fig. 1b, FDR < 0.05). Interestingly, although males to females comparison (M vs. F) revealed 2022 DMS, only 20 sites overlapped with the pathology comparison (TD vs. WS) and were removed from the final analysis (Supplementary Fig. 1). We did not identify DMS in the age comparison.

Next, we performed genomic annotations (via HOMER tools) to DMSs and allocated them to promoters, exons, introns, intergenic, 5' and 3' UTR loci (Fig. 1c left panel). Notably, some DMSs were not localized to these specific genomic loci and thus excluded from this analysis (Supplementary Table 2). Furthermore, we assessed DMSs distribution by normalizing them to the number of general CpG island in each genomic loci (Fig. 1c right panel) [77]. While Hypo-DMSs are predominantly annotated as promoter sites, the vast majority of Hyper-DMSs are annotated as introns and intergenic loci (Fig. 1c).

As compared to DMSs, DMRs, corresponding to multiple consecutive methylated CpG sites, are considered to be more stable and heritable [78]. As such, we investigated DMRs in individuals with WS and their TD controls and identified 319 DMRs (Fig. 1d). Similarly, comparison of sex and age as variants revealed 113 DMRs in M vs. F and 5 DMRs in younger vs. older. Only 4 DMRs

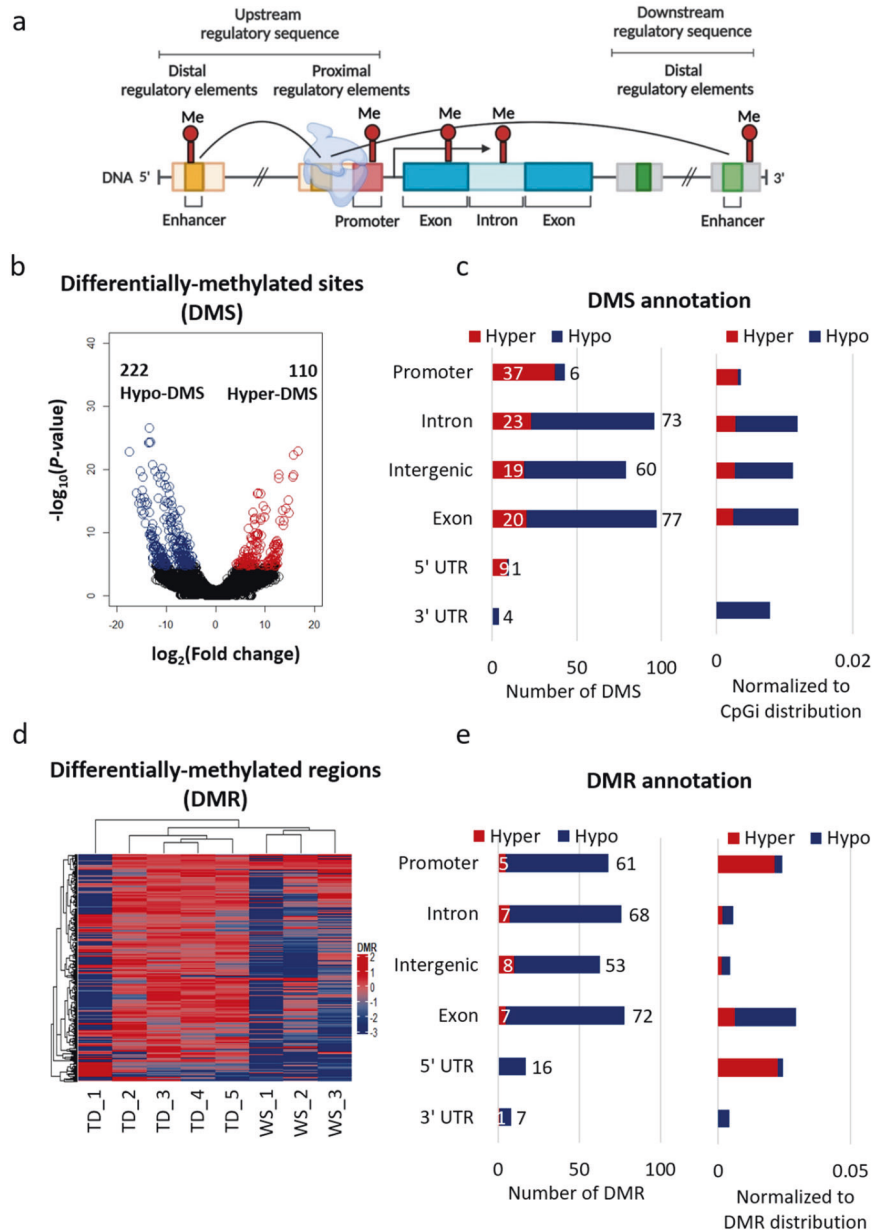


Fig. 1 7q11.23 deletion promotes genome-wide aberrations in the human frontal cortex DNA methylation landscape. **a** Schematic diagram of a methylated gene and regulatory elements. **b** DMSs are shown as a volcano plot. Values of methylation from pairwise comparisons (\log_2 -fold change) were plotted against the average $-\log_{10}(P\text{-value})$. Differentially hypo-methylated DMSs are shown in blue, differentially hyper-methylated DMSs are in red, and non-significantly methylated CpG sites are shown in black. $FDR < 0.05$, $WS\ n = 3$, $TD\ n = 5$. **c** Genomic distribution of Hypo- and Hyper-DMSs, as determined by HOMER to promoters, introns, intergenic, exons, 5' and 3' UTR regions (left panel). Comparison of DMSs distribution to the general occurrence of DNA methylation in the human brain. Ratio values were calculated by dividing the number of DMSs by the number of identified CpG islands for each genomic location (right panel). **d** DMRs are presented in a heatmap. Average methylation levels (\log_2 -fold change) in individuals with WS were compared with those of TD individuals. **e** Genomic distribution of Hyper- and Hypo-DMRs (left panel). Comparison of DMRs distribution to the general occurrence of DNA methylation in the human brain. Ratio values were calculated by dividing the number of DMRs by the number of identified CpG sites for each genomic location (right panel).

overlapped with the TD vs. WS comparison and were therefore excluded from the final analysis (Supplementary Fig. 1, Supplementary Table 3). Surprisingly, unlike DMSs, DMRs were mostly found to be hypo-methylated (henceforth termed Hypo-DMRs) (Hypo-DMRs = 287/Hyper-DMRs = 28) in individuals with WS, with promoters, gene exons and 5' UTR being over-represented in this group (ratio values calculated by normalizing them to the number of general DMRs distribution in the human brain [79] Fig. 1e).

Accumulating evidence indicates that DNA methylation can significantly modify transcriptional regulation by altering TF

binding. Thus, further functional insight was gained by assessing TF-binding motif sequences adjacent to DMSs (Fig. 2a) and DMRs (Fig. 2b) using HOMER [80]. Our analysis revealed that in individuals with WS, several motifs within TF-binding sites were differentially methylated, as compared to TD controls. Among the binding sites affected were those for TFs involved in cell differentiation and proliferation (*i.e.*, ZFP105, SCRT1), activators of the dopamine transporter (*i.e.*, ZFP161) and cognitive disability (*i.e.*, SOX8, JUN). Notably, the affected *GTF2B*-binding motif might be associated with the *GTF2I* gene deleted from the WSCR locus in

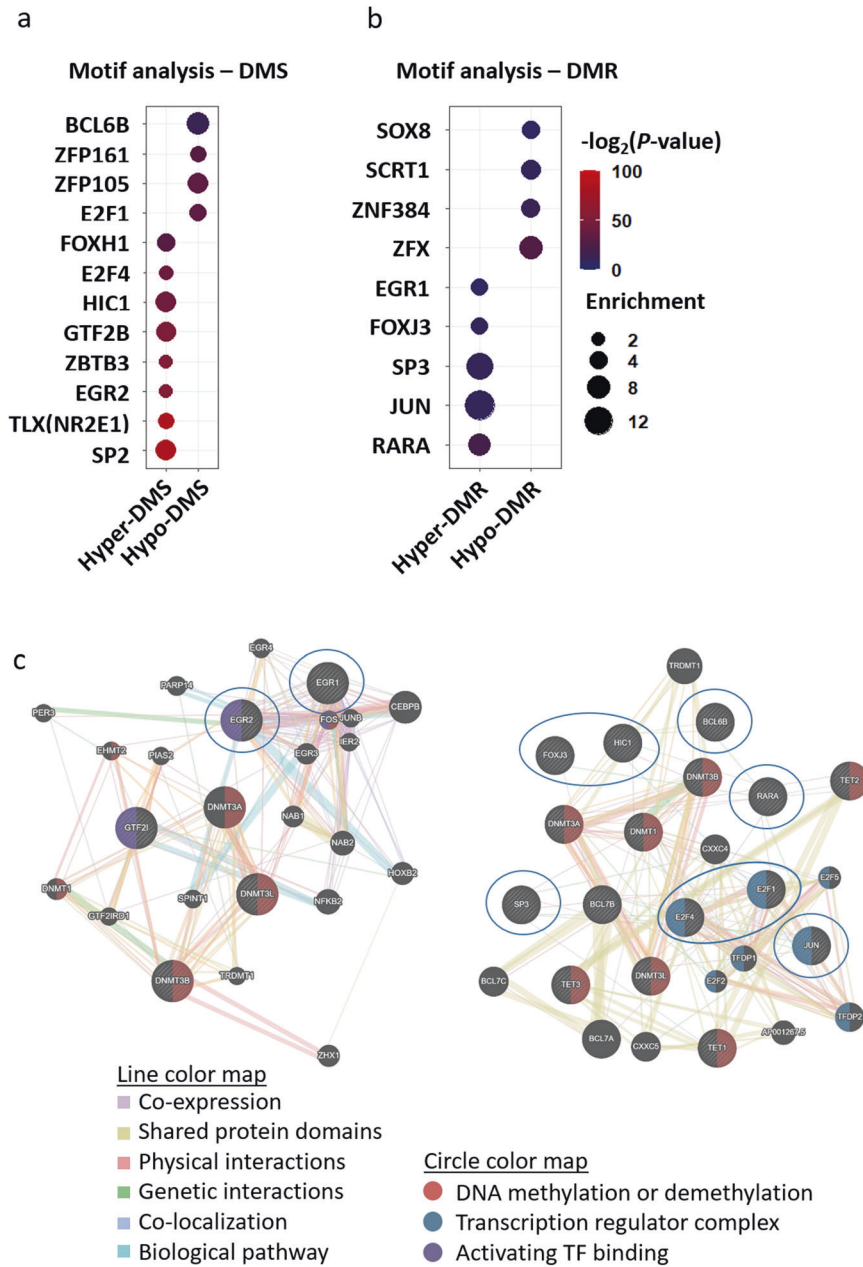


Fig. 2 The association between 7q11.23 deletion, aberrant DNA methylation and TF binding. TF-binding motif enrichment in **a** DMSs ($-/+$ 25 bp) and **b** DMRs. The size of the circle indicates the level of DMS/DMR site enrichment. Different colors indicate different $-\log_2(P\text{-value})$, as indicated in the scale bar. **c** Association network analysis. Diagrams represent two sub-networks between the TF-binding motifs identified in DMSs/DMRs (marked by blue ovals), genes commonly deleted in WS, and common epigenetic modifiers that alter methylation. The analysis was performed using GeneMANIA.

individuals with WS [81, 82]. We also found the *EGR2*-binding motif to be highly enriched in DMSs (Fig. 2a). *EGR2* (early growth response 2, also called KROX20) is known to mediate the transcription of various genes related to neuronal development and plasticity, cognition, circadian rhythm, and social behaviors [83–86]. The list of DMSs also included the *TLX* gene that encodes for an orphan nuclear receptor, also named NR2E1 (nuclear receptor subfamily 2, group E, member 1) that is predominantly expressed in the central nervous system (CNS) [87, 88]. Deletion of *TLX* impaired adult hippocampal neurogenesis, as well as motor, cognitive and anxiety-related behaviors, all of which are associated with several human mental illnesses, such as schizophrenia and bipolar disorders [89, 90]. We also identified enriched TF-binding motifs on hyper-DMSs (Fig. 2b), such as *EGR1*, *SP3* and

JUN, genes that were previously associated with neuronal plasticity, synaptic function and cognition [66, 91].

Next, we considered possible links between the TF-binding motifs identified in DMSs/DMRs (Fig. 2a, b), specifically in common modifiers that alter DNA methylation (e.g., in genes for DNMT and TET family members) and genes commonly deleted in individuals with WS, using the GeneMANIA interface. The TF-binding motifs identified in DMSs/DMRs are marked by blue circles (Supplementary Fig. 2). GeneMANIA builds and uses weighted interaction networks from various data sources (e.g., real-valued protein physical interaction networks, gene profile datasets and multi-sample microarray expression) and is able to process user data into these networks. Our analysis revealed co-expression and physical interactions between GTFIIH and the DNA

methyltransferase 3 beta (DNMT3B) and 3 alpha (DNMT3A) (Fig. 2c, left panel). Moreover, our analysis revealed co-expression and physical interactions between DNMT3A and EGR2, which were identified by HOMER in the motif analysis (Fig. 2c, left panel).

Finally, our GeneMANIA association network analysis revealed potential interactions between DNMT1/TET family members, several TFs (namely, HIC1, E2F4, E2F1, JUN and SP3) and the *BCL7B* gene (which is deleted in WS) (Fig. 2c, right panel). Collectively, these results support the notion that genes in the WSCR serve as scaffolds for epigenetic modulators, such that deletion of these genes has the potential to disrupt the proper binding of several TFs and lead to genome-wide epigenetic and transcriptional aberrations.

Aberrant methylation of regulatory elements and their target genes following 7q11.23 deletion

To date, numerous studies have focused on alterations in the methylation of exons and promoters which are tightly linked to changes in gene expression [22, 23, 92–94]. Still, the functional roles of differential methylation of REs, DNA sequences typically found in introns and intergenic regions, remain poorly understood. It is notable that REs act independently of the distance and orientation of their target genes by forming three-dimensional (3D) chromatin loops in a cis- or trans-manner. This chromatin configuration brings REs into physical contact with the promoters of genes they affect, a process also known as enhancer–promoter interactions [95] (Fig. 3a). New approaches, such as chromosome conformation capture (3C) techniques [96], offer new tools to map 3D chromatin contacts on a genome-wide scale and accurately link REs to their respective genes (Fig. 3a).

We first used HOMER annotation tools (default; the nearest gene) to recognize DMSs/DMRs. In this manner, we identified 104 genes with promoters and 136 exons with altered methylation (Fig. 3b, Supplementary Table 4). In some cases, we found several changes in methylation of the promoter or exons of the same gene; these were counted as a single occurrence.

To further address the functions of DNA methylation of intronic and intergenic loci, we examined previously published data to assess the overlap of DMS/DMRs with two specific markers of enhancers, namely, acetylation of histone H3 Lys27 (H3K27ac) and mono-methylation of histone H3 Lys4 (H3K4me1) [97]. We identified a ~67% overlap between DMSs/DMRs and H3K27ac/H3K4me1 modifications (Supplementary Fig. 3), confirming that most of these loci function as active enhancers in the human brain. Next, by consulting cell type enhancer–promoter interactome data (merged all cell types interactions together) from Nott et al. [28], we accurately mapped DMSs/DMRs found within enhancers onto their respective target genes. Such analysis yielded a list of 68 gene candidates that potentially could be altered by aberrant methylation of putative REs (33 genes from intergenic regions and 35 from introns loci; Supplementary Table 4). Here too, multiple methylation sites in the same intron or intergenic region were annotated to the same gene and counted as a single occurrence. All annotated genes (from HOMER and interactome maps) from DMS/DMRs are presented in Fig. 3b and Supplementary Table 4.

To better understand gene networks and biological processes that might be altered by aberrant methylation in individuals with WS, we next performed a gene ontology (GO) analysis of hyper- and hypo-DMSs/DMRs (Fig. 3c, Supplementary Table 5). Our results indicated that hyper-DMSs/DMRs were significantly enriched in pathways such as ‘nervous system development’ and ‘trans-synaptic signaling’ with genes such as *PLAGL1*, *SOX11* and *HOXA2* being affected (Fig. 3c, Supplementary Fig. 4a and b). Moreover, we identified several genes, such as *LINGO1*, that harbor both hyper- and hypo-methylation in their vicinity, with the potential to affect their transcription level in an opposite manner (Supplementary Fig. 4c). Hypo-DMSs/DMRs were significantly enriched in pathways such as ‘oligodendrocyte specification and differentiation’, ‘dopaminergic neuron differentiation’, ‘axon guidance’, ‘cognition’, and

‘MAPK cascade’, with genes such as *ID4*, *LINGO3*, *GAD1*, *GPR17* being affected (Fig. 4a, Supplementary Fig. 5).

We next sought to assess the potential effects of differential methylation on global gene expression. Thus, correlation analysis was performed between differential DNA methylation and differential expressed genes (DEGs) in (i) brain samples from individuals with WS compared to TD controls [21], (ii) brain samples from individuals with ASD compared to TD controls [98], (iii) neural progenitor cells (NPCs) and neurons derived from fibroblasts of individuals with WS compared to TD controls [99] and (iv) brain samples from mice with *Gtf2i* neuronal deletion from forebrain (referred herein as *Gtf2i* cKO mice), compared to controls [21] (GeneOverlap, Fisher’s exact test for *P*-value and odds ratio). Our analysis revealed a significant correlation between hypo-methylated sites in individuals with WS compared to TD controls and up-regulated transcripts in brain samples from individuals with WS compared to TD controls and individuals with ASD compared to TD controls (Fig. 3d, *P*-value = 0.027, *P*-value = 0.014, respectively). Interestingly, these correlated transcripts were specifically associated with OL specification/differentiation (*i.e.*, *LINGO3*, *MBP*, *SEMA3B*, *OLIG1*, *GAD1* and *GPR17*, Supplementary Table 6). These data suggest that common pathophysiological deficits are involved in WS and ASD that are related to neuronal and OL functionality. Furthermore, our correlation analysis showed that clusters of DEGs in NPCs and neurons derived from WS iPSC compared to TD controls were predominantly correlated with hypo-methylated sites in individuals with WS compared to TD controls (Fig. 3d) and play a role in transcriptional regulation (*i.e.*, *HIC1*, *SP6*), axonal function (*i.e.*, *SEMA3B*) and structural component of neurons (*i.e.*, *MYL9*). Notably, several DEGs in *Gtf2i* cKO mice compared to controls, were also correlated with hypomethylated sites in our current study, such as *Lingo3* (Fig. 4b). These data further strengthen our hypothesis that *Gtf2i* neuronal deletion might lead to alterations in the epigenome and represent some of the pathological manifestation seen in individuals with WS.

Genes involved in social behavior, myelination and glia differentiation present abnormal methylation patterns in individuals with WS

Our data suggest that aberrant methylation of REs in individuals with WS might lead to specific transcriptional dysregulation (*i.e.*, *ID4*, *GAD1*, *GPR17*, *LINGO1*, *LINGO3*). These genes are of special interest due to their central roles in mediating features known to be affected in WS, especially in key processes, such as myelination, brain development and social behavior.

In the next step, we wanted to determine whether changes in methylation of REs affect gene expression in our datasets. Thus, different cohort of frontal cortex (BA9) sections from the same individuals with WS (*n* = 3) and TD controls (*n* = 5) used for the RRBS study, were subjected to quantitative polymerase chain reaction (qPCR) with designated primers for *ID4*, *GAD1*, *GPR17*, *LINGO1* and *LINGO3*.

Importantly, since several methylated sites on RE were found to be in opposite orientation or kilobases away from their target genes (*i.e.*, *GPR17*, *LINGO1*), the same samples were subjected to 3C assays followed by qPCR (3C-qPCR) with designated primers aligning to the promoter sites of and to the methylated RE. Due to the small sample size, we wanted to further validate our results, and thus we also tested the expression of these genes in *Gtf2i* cKO mice.

Consistent with the observed aberrant hypo-methylation on genes promoter (Supplementary Fig. 5a and c), our analysis revealed significant increase in *ID4* (*p* = 0.047) and *GAD1* (*p* = 0.006) mRNA levels in WS, as compared to TD controls (Fig. 4a). Similarly, *Gtf2i* cKO mice showed a significant increase in *Id4* mRNA level (*p* = 0.0003) but not in *Gad1* transcripts (Fig. 4b).

Hypo-methylation on the intronic part of *LINGO3* was correspondingly associated with higher levels of mRNA levels in both WS patients (*p* = 0.015) and *Gtf2i* cKO mice (*p* = 0.0003), compared to matching controls (Fig. 4a, b).

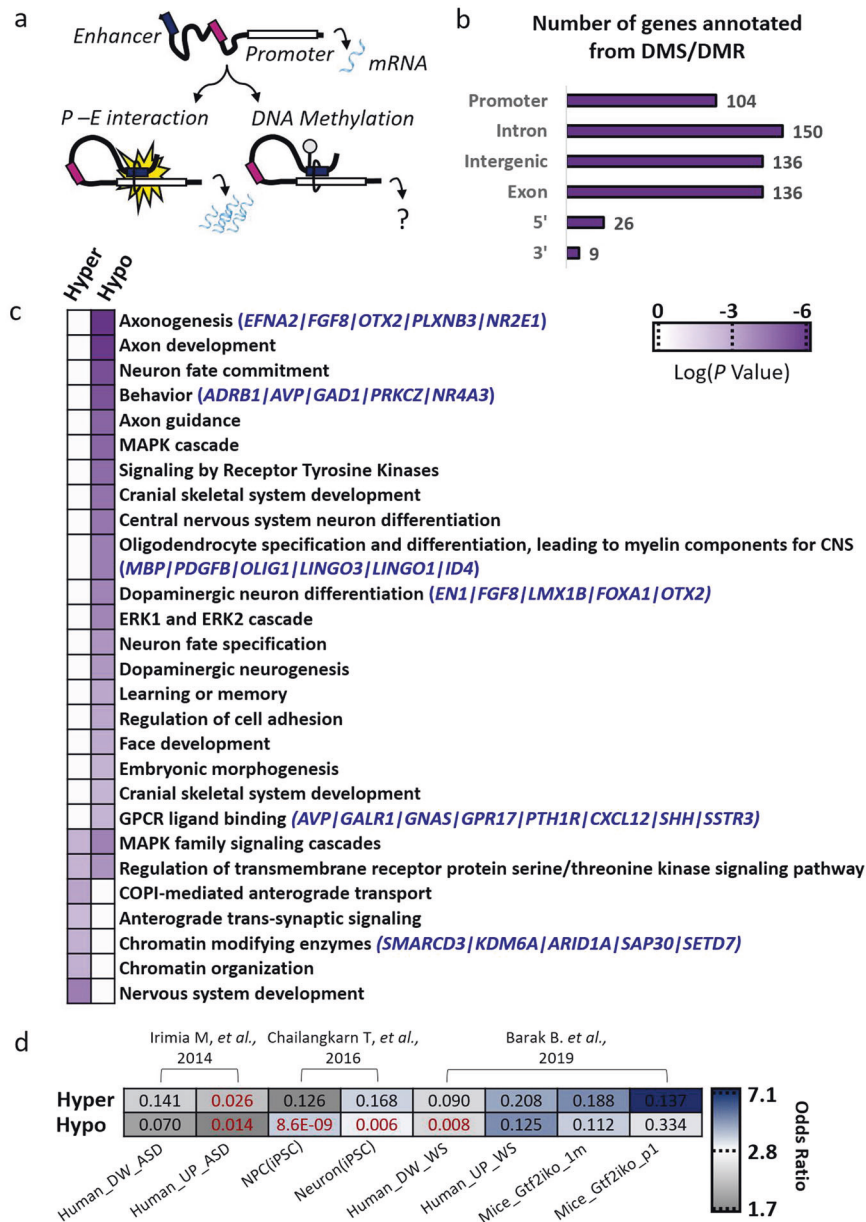


Fig. 3 Consulting the human brain interactome to map aberrant methylation of regulatory elements and their target genes. **a** Proposed model for methylated REs in which distal RE sequences are separated from promoters, such that the rate of transcription is reduced. Loop formations that enable physical proximity between REs and a promoter region enable RNA polymerase II (RNAPII) complexes to bind and up-regulate transcription. DNA methylation of distal REs can disturb loop formation and alter transcription. **b** Annotation analysis. DMSs/DMRs in promoters, exons, 3' and 5' UTRs were annotated to genes using HOMER tools. In addition, DMSs/DMRs in introns and intergenic regions were mapped to their target genes by enhancer-promoter interactome data from Nott et al. 2019. **c** Gene ontology (GO) analysis of Hyper- and Hypo-DMSs/DMRs with a list of representative genes assigned to different pathways. GO analysis was performed using Metascape and values are presented in log(*P*-value) scale. **d** Correlation analysis was performed between differential DNA methylation and differential expressed genes (DEGs). Transcriptional data were taken from (i) brain samples from individuals with WS [21] or autism spectrum disorder (ASD) [98], (ii) neural progenitor cells (NPCs) and neurons derived from WS fibroblasts [99] and (iii) brain samples from mice with *Gtf2i* deleted from excitatory neurons [21] and their controls. *P*-value (presented in numbers) and odds ratio (color scale) from Fisher's exact were calculated by GeneOverlap package and presented in the heatmap.

Next, we characterized transcription regulation properties in two genes of interest, *GPR17* and *LINGO1*, which were associated with altered methylation on RE (Fig. 3b, Fig. 4a, Supplementary Table 4). To achieve this, we first performed 3C-qPCR assay to measure long range interaction frequency between the gene's promoter and the predicated hyper- or hypo-methylated RE (Fig. 4c, d). These loci were compared to control sites at a similar distance and in opposite orientation. Consistent with the significant transcriptional increase in *GPR17* level in individuals

with WS compared to TD controls ($p = 0.035$, Fig. 4a), we identified a significant interaction between proximal (~5 kb) hypo-methylated site and the *GPR17* promoter (Fig. 4c). Similarly, we identified a significant interaction (measured above control loci) between the *LINGO1* gene's promoter and the hyper-methylated RE (Fig. 4d). Together, these results further support the idea that altered genetics may not be the sole contributor to the WS pathology, and suggest that transcription regulation might be predisposed by epigenetic modifications in WS.

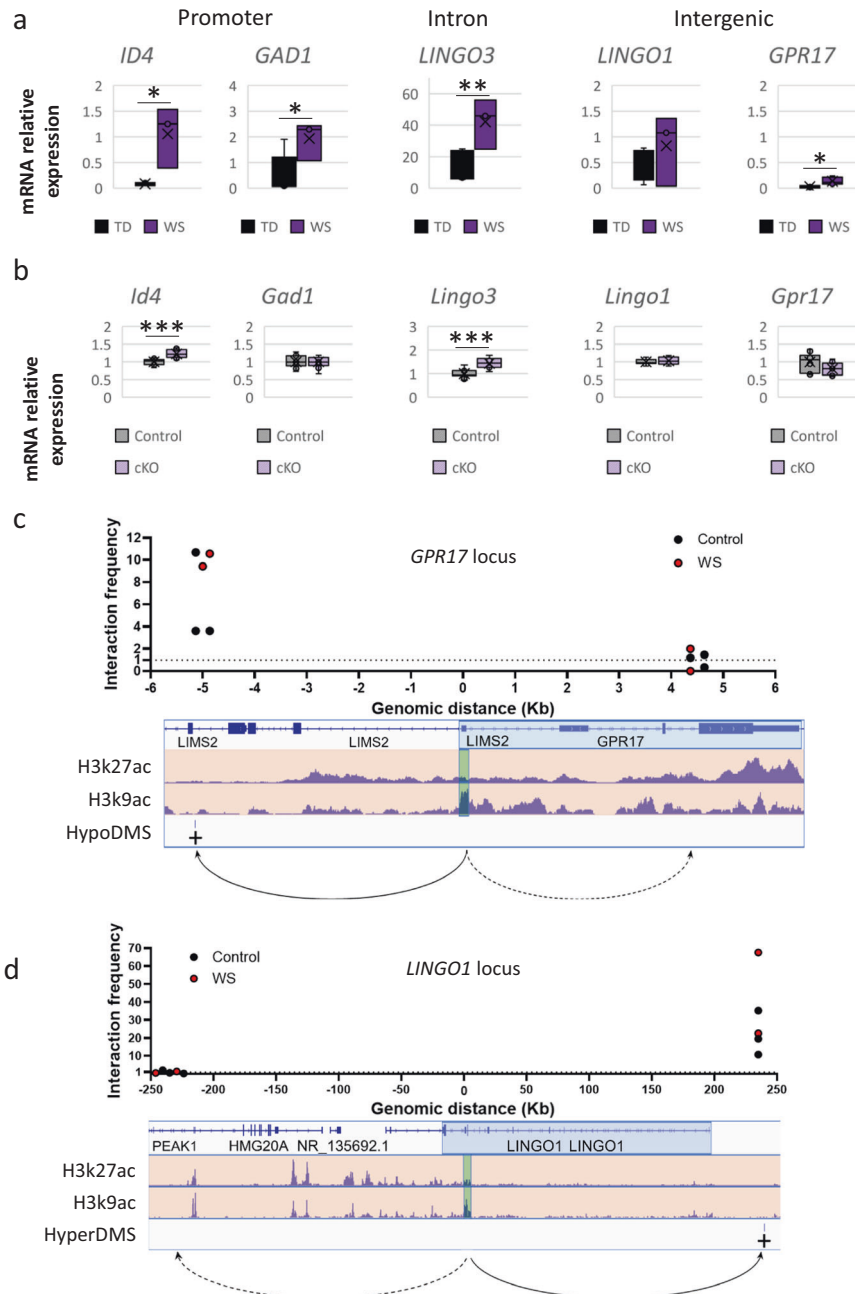


Fig. 4 Abnormal methylation patterns in individuals with WS are associated with genes involved in myelination and glia differentiation. RT-qPCR of representative mRNAs (*ID4*, *GAD1*, *LINGO3*, *LINGO1*, *GPR17*) from **a** individuals with WS, compared with those of TD controls and **b** *Gtf2i* cKO mice, compared to controls. mRNA expression is relative to tubulin. 3C-qPCR assay at the **c** *GPR17* or **d** *LINGO1* locus. Interaction frequencies between methylated –REs (hypo or hyper, respectively) and promoter regions were assessed, relative to random genomic loci at similar distance from the promoter region. Promoter regions are demarcated by green rectangle. Coding sequences are demarcated by light-blue layer on top of the hg38 human genome track. IGV genome browser tracks presenting H3K27ac, which demarcate active enhancers and promoters and H3K9ac peaks, which demarcate only active promoters. Fold ratio of interaction frequencies between methylated –REs and promoters region is relative to interaction frequencies at random genomic loci, as indicated by the dotted line (*i.e.*, set as 1). Data are shown as mean \pm s.e.m. **a** $n = 5$ TD controls, $n = 3$ WS. **b** $n = 9$ *Gtf2i* cKO mice, $n = 11$ control mice. **c, d** $n = 3$ TD controls, $n = 2$ WS. * $p < 0.05$, ** $p < 0.01$, *** $p < 0.005$ *t*-test.

Cell type-specific methylation analysis reveals aberrant patterns in individuals with WS, predominantly in active enhancers of neurons

Epigenetic modifications can be tissue-specific and play key roles in development of the mammalian nervous system [100–102]. Importantly, emerging evidence suggests that the activity of REs can be restricted to a particular tissue, cell type, or even to specific physiological, pathological or environmental conditions. To study

this, we utilized previously published datasets from Nott et al., which defined active promoters and enhancers for major human brain cell types [28]. This work provided us with resources to examine cell-type specific patterns of methylation enrichment, and to elucidate possible cell-type gene network deficiencies in individuals with WS, as compared to TD controls.

For such analysis, we overlapped DMS/DMR location with loci that were defined [28] as active promoters, enhancers or super-

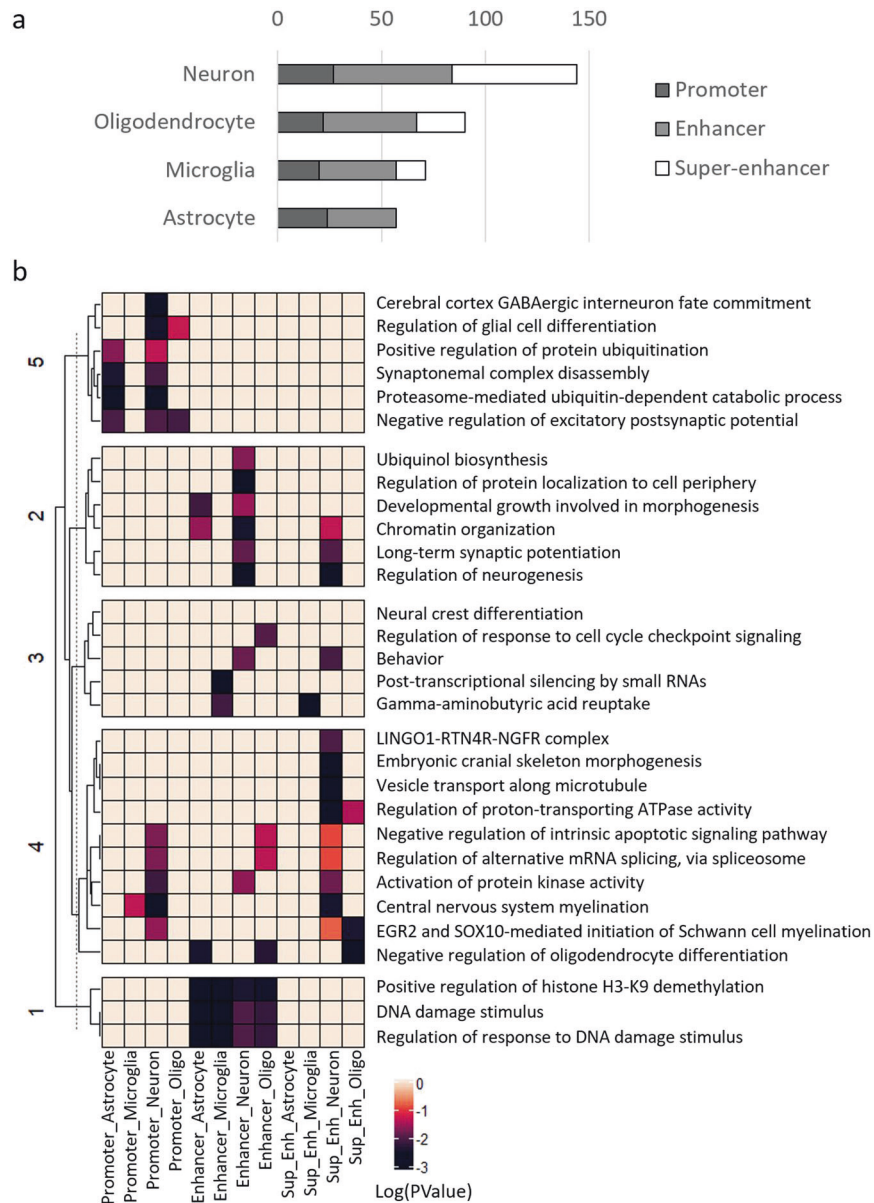


Fig. 5 Cell type-specific methylation analysis reveals aberrant patterns in individuals with WS, predominantly in active neuron enhancers. **a** Genomic distribution of DMSs/DMRs over four major cell types. Methylated sites were overlapped with loci that were defined as active promoters, enhancers or super-enhancers (as defined by Nott et al. [28]), in four major cell types, namely, neurons, OLs, microglia and astrocytes. **b** GO analysis (Metascape) of genes whose promoters, enhancers and super-enhancers are enriched in the four major cell types considered. Values are presented in log(P -value) scale. Gene sets were clustered according to the k-means function.

enhancers, in four major cell types, namely, neurons, OLs, microglia and astrocytes. Our data showed that aberrant methylation in individuals with WS was mostly abundant in enhancers and super-enhancers (corresponding to regions of the mammalian genome comprising multiple enhancers in close genomic proximity [103]), that are predominantly active in neurons (Fig. 5a). We also observed that OLs were the cell type second-most affected by abnormal methylation (Fig. 5a). Neurons and OLs share a reciprocal signaling relationship, whereby neurons send signals to OPCs and OLs to direct their proliferation, differentiation and myelination. Reciprocally, OLs shape neuronal axon structure and conduction as OLs extend multiple processes that ensheath nearby axons in layers of myelin to support proper brain development and function [104–106].

Given these results, we next performed GO analysis of genes whose promoters, enhancers and super-enhancers were enriched

in the above-mentioned cell types (Fig. 5b; top GO pathways are reported in Supplementary Table 7). Gene sets were unbiasedly clustered (k-means function) based on their log(P -value) enrichment patterns. In individuals with WS, as compared to TD controls, aberrant methylation of neuron and astrocyte promoters (cluster 5) was highly enriched in components of pathways associated with ‘synaptonemal complex disassembly’, ‘negative regulation of excitatory postsynaptic potential’ and ‘protein ubiquitination’. Surprisingly, pathways associated with myelination processes (i.e., cluster 4, ‘EGR2 and SOX10-mediated initiation of Schwann cell myelination’, ‘negative regulation of oligodendrocyte differentiation’) were primarily enriched in neurons and OL enhancers/super-enhancers. These results are consistent with our previous results showing that deletion of *Gtf2i* in excitatory neurons led to reductions in myelin-related gene transcript levels, OL numbers, neuronal myelination and function [21] and white matter

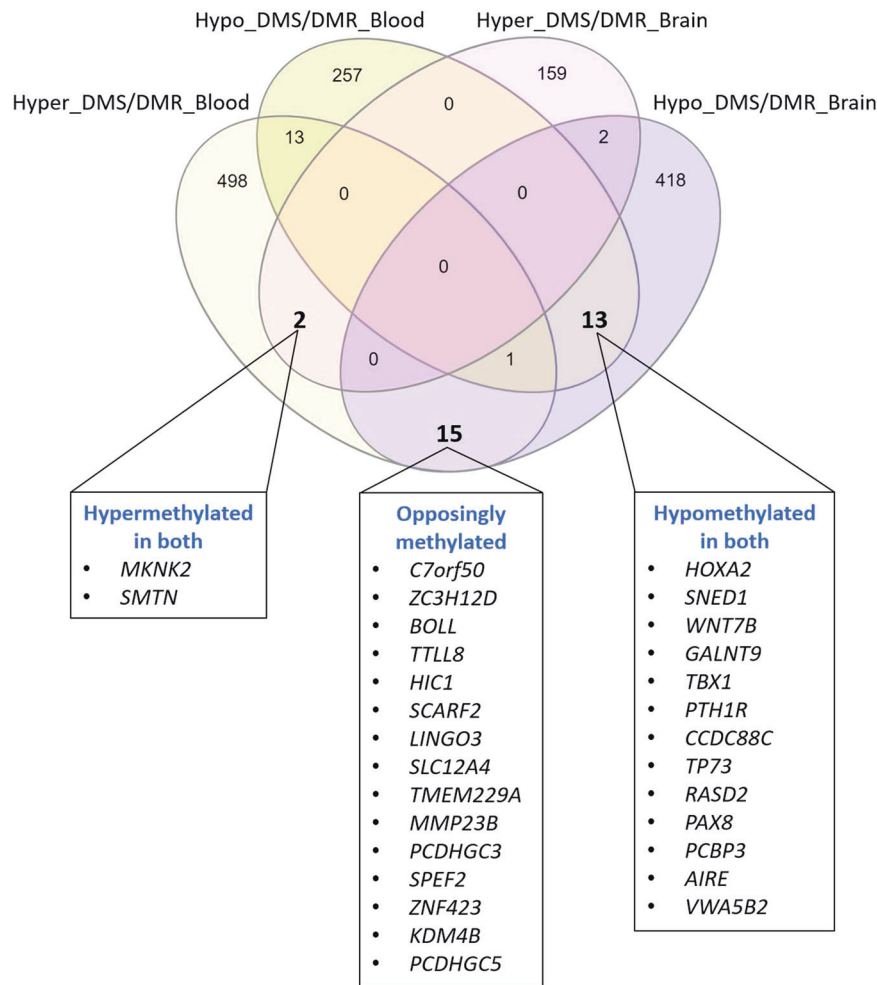


Fig. 6 A comparison of methylated risk loci between brain and blood samples from individuals with WS identified three major gene clusters. Overlap of DNA methylation profiles from blood samples [22, 23] and frontal cortex samples derived from individuals with WS. InteractiVenn (a web-based tool for the analysis of sets drawn as Venn diagrams) was utilized to identify overlaps between names of annotated genes and DMSs/DMRs. Three major clusters were identified; (i) A hyper-methylated cluster comprising genes hyper-methylated in both blood and brain samples; (ii) a hypo-methylated cluster comprising genes hypo-methylated in both blood and brain samples; and (iii) an oppositely methylated cluster comprising genes that were oppositely methylated.

properties [24, 25]. Our data also highlighted specific pathways that might be impaired in OLs (Fig. 5b), such as ‘kinase activity’ (cluster 4), which was previously mentioned as one of the main signaling pathways for OPC proliferation and differentiation into mature myelinating OLs, and for myelin production [107–111]. In agreement with our previous publication [21], these data support the notion that OPC differentiation might be impaired by 7q11.23 deletion.

Together, these data imply the importance of proper neuron-glia interactions that promote myelination and which could be impaired in WS individuals. Last, aberrant methylation patterns common to enhancers of all the major cell types considered here (cluster 1), as seen in individuals with WS, were associated with biological processes involved in epigenetic modification (H3K9 dimethylation) and the DNA damage response (Fig. 5b).

Examination of methylated risk loci from individuals with WS identified three major gene clusters with differential association between brain and blood samples

Lastly, we addressed previously published DNA methylation profiles from blood samples derived from individuals with WS [22, 23] and overlapped such profiles with those from the frontal cortex samples we studied here (Fig. 5), given how such analysis

could promote efforts to discover potential novel biomarkers for WS in peripheral blood and thus expand our understanding of endophenotypes associated with WS. Despite the relatively overall low correlation between DMS/DMR loci, we identified a few candidate genes with high association between brain and blood samples. Specifically, we identified 3 major clusters: (1) A hyper-methylated cluster comprising genes hyper-methylated in both blood and brain samples (*i.e.*, *MKNK2* and *SMTN*); (2) a hypo-methylated cluster comprising genes hypo-methylated in both blood and brain samples; and (3) an oppositely methylated cluster comprising genes that are oppositely methylated (Fig. 6).

The hypo-methylated cluster includes the transcription regulator *HOXA2*, which is spatially and temporally regulated during embryonic development [112, 113]. This gene is located on chromosome 7 and is involved in the placement of hindbrain segments in the proper location, as well as skeleton morphology [114, 115]. This pattern of expression and epigenetic regulation suggests that *HOXA2* could be a potential biomarker for WS. These results from brain tissue and blood samples support a model whereby hypo-methylated sites can lead to up-regulation of the relevant transcripts and thus lead to inhibition of cell proliferation.

Of the genes in the oppositely methylated cluster, we identified *TTLL8*, which encodes Tubulin Tyrosine Ligase-Like Protein 8, an

enzyme from the tubulin-tyrosine ligase-like (TLL) family that play essential roles in the post-translational modification of tubulin in mammals [116, 117]. These and other post-translational modifications are vital for the formation and maintenance of the polarized morphology of neurons. Our results showed *TLL8* to be hypomethylated in the brains of individuals with WS, as compared to TD controls, and thus could be up-regulated in WS, which could, therefore, lead to altered brain development.

DISCUSSION

Several studies indicated that transcriptional programs might be predisposed to epigenetic changes, leading to WS pathology. This notion was strengthened by studies that showed genome-wide transcriptional aberration in blood cells and brain samples that extended beyond the WSCR locus [22, 23]. Moreover, deleted genes from the 7q11.23 region (such as *GTF2I*) are capable of interacting with epigenetic modifiers from the DNMTs and TET families, and thus play key roles in determining the cellular epigenetic landscape.

To describe possible effects of 7q11.23 deletion on the brain epigenome, we examined patterns of DNA methylation in brain sections from frontal cortex of individuals with WS and TD controls. Our data revealed vast changes in the methylome of individuals with WS, as compared to TD controls, predominantly in REs. Motif analysis identified two major TFs involved in neuronal development assigned to the list of hyper-DMSs and could thus lead to their decreased binding. The first is *EGR2* (Fig. 2a), which participates in the transcription of several genes important to neuronal development, cognition, circadian rhythm, social behavior, plasticity and myelination, including *MBP*, *SOX10* and *MAG* [83–86, 118–120]. *EGR2* was reported to be critically important in myelination in the early stages of development of peripheral nerves, while mutated *EGR2* has been identified in several myelin disorders [86, 121]. *EGR2* was found to repress genes during peripheral nerve myelination, among them being the TF *ID4* [118, 122, 123]. Previous analysis of blood samples from individuals with WS [22, 23] also revealed enrichment of several TFs, including *EGR2*. Interestingly, association networks analysis (Fig. 2c) predicted potential physical interactions among *EGR2*, *GTFII-I* and *DNMT3B*, through *DNMT3L* [45]. *DNMT3B* is a DNA methyltransferase required for genome-wide *de novo* methylation and is essential for mammalian development [124]. This methyltransferase interacts with TFs to promote DNA methylation at specific sites and can interact with *GTFII-I* and *EGR2* through a linker protein called *DNMT3L*, a DNA-methyltransferase 3-like protein [45]. As noted above, the TF *EGR2* plays a pivotal role in brain development and myelination [84–86]. Thus, it is conceivable that *GTF2I* deletion affects the dynamics of interaction with *DNMT3L*, thereby perturbing the methylation landscape, and subsequently altering downstream activation or binding of other TFs, such as *EGR2*. The pool of hyper-methylated *EGR2* in WS brains, as compared to TD controls, could explain the misregulation of genes important for myelination processes, which, in turn, could lead to the myelin deficits described in our previous work [21].

The second TF to be differentially methylated in individuals with WS, as compared to TD controls, is *TLX*, which is predominantly expressed in the central nervous system [87] and was found to play an essential role in neurogenesis during early embryogenesis and to perform crucial functions in regulating adult neural stem cell proliferation and differentiation [87, 88]. Interestingly, deletion of *Tlx* in mice was shown to impair adult hippocampal neurogenesis, and affect motor, cognitive and anxiety-related behaviors [90], while deficits in *TLX* are associated with several human mental illnesses, such as schizophrenia and bipolar disorders [89]. WS is mainly characterized by cognitive and behavioral abnormalities, anxiety, hyper-sociality and intellectual

disability. The hyper-methylation of *TLX* motifs in WS tissue samples may explain some of these features. Furthermore, we identified an enrichment of TF-binding motifs on hyper-DMRs (Fig. 2b), such as those that bind *EGR1*, *SP3* and *JUN*, which were previously associated with neuronal plasticity, synaptic function and cognition [66, 91], and thus might impair the proper function of neurons in individuals with WS, as compared to TD controls.

A growing body of literature based on studies conducted in different animal models, tissues and cell types has reported differential methylation not only on gene promoters but also in intergenic regions, introns and other non-coding DNA regions [125–129], which are capable of interacting with their respective genes in the three-dimensional space. In this context, a considerable number of identified DMR/DMSs were located in introns and intergenic loci (Fig. 1c). Hence, to accurately link DMSs/DMRs on enhancers to their target genes, and to assess the potential effects of such methylation on transcription, we utilized previously published human brain three-dimensional chromatin contact maps [96]. Such analysis underscores how important regulatory sites can be located as far as mega-bases from the genes they affect, can be in the opposite orientation to such genes, and can affect multiple genes at the same time (Fig. 1a). Moreover, enhancers might also harbor binding sites for transcriptional repressors, such that methylation of these sites might, in turn, lead to up-regulation of gene expression. Collectively, these data reveal another level of complexity and further emphasize the need to study interactions between chromatin folding and the epigenome, and the effects of such interactions on transcription and brain functionality.

Consistent with the myelination deficits, abnormal gene expression and behavioral phenotypes presented in WS [21, 24], both hyper- and hypo-DMSs/DMRs were enriched in gene pathways related to 'nervous system development', 'oligodendrocyte specification and differentiation', 'trans-synaptic signaling' and 'learning and memory'. Specifically, we identified hypomethylation of *ID4* and *LINGO3* in individuals with WS as compared to TD controls, which were previously shown to affect neuronal development and myelination [72–75, 130–135]. *ID4* is a potent inhibitor [72, 130–132, 136] of gene transcription that can affect cell type-specific gene expression during cell commitment and differentiation [136, 137]. Specifically, *ID4* was found to be crucial for peripheral nerve myelination, as it can increase OPC proliferation and maintain the cells in their undifferentiated state [72, 134, 136–139]. Interestingly, *EGR2*, binding sites for which were enriched in our TF-binding motif analysis, was found to down-regulate *ID4* expression levels. Thus, hypomethylation of *ID4* can lead to its over-expression, as compared to TD controls, which may cause inhibition of OPC differentiation in the frontal cortex of individuals with WS, resulting in myelin impairment, as shown in our previous work [21]. Similarly, *LINGO1*, a transmembrane protein selectively expressed in neurons and OLs, is also characterized as a negative regulator of neuronal survival and axonal regeneration and inhibits OPC differentiation into mature myelinating OLs [74, 75, 133]. *LINGO1* and its homolog *LINGO3* are co-expressed in the brain and physically interact with each other [73]. Thus, *LINGO3* hypomethylation leads to its over-expression, as compared to TD controls (Fig. 4a), which may also result in inhibition of OPC differentiation and decreased myelination.

GAD1 encodes for the *GAD67* protein, a key enzyme in the synthesis of the neurotransmitter gamma-aminobutyric acid (GABA). Changes in DNA methylation and reduced chromatin accessibility of *GAD1* were previously shown to decrease *GAD67* protein levels in the prefrontal cortex of individuals with schizophrenia [140, 141]. We demonstrated hypomethylation of *GAD1* in brain tissues of individuals with WS (Supplementary Table 3). This may lead to *GAD67* over-expression, relative to TD controls, possibly indicative of increased inhibitory activity in the prefrontal cortex of individuals with WS. This could lead to an

altered excitatory/inhibitory balance (known as E/I imbalance) that can affect social behavior [4, 142–144].

We, moreover, identified gene networks that are associated with ‘MAPK family signaling cascades’ as being altered in WS, as compared to TD controls [145]. The proliferation, differentiation and maturation of OPCs into mature myelinating OLs, as well as the myelination process itself, rely on the MAPK pathway [107–111]. One of the TFs that is activated by the MAPK pathway is LINGO1, which is expressed in both axons and OLs [75, 146], which, through the MAPK-RhoA signaling pathway, can inhibit OPC differentiation and thus, potentially decrease myelination. Together, these aberrant methylation patterns may alter OPC differentiation, OL maturation and neuronal myelination. Abnormal methylation was also found in the gene encoding for the G-protein-coupled receptor 17 (GPR17), an OL-specific receptor that is expressed transiently in late stage OPCs/early differentiated OLs, and shown to regulate OPC differentiation [147, 148]. It was indicated that GPR17 can strongly inhibit OPC differentiation and maturation, and that it is associated with an increase in ID2/ID4 expression and nuclear localization, all of which can lead to abnormal myelination. Together, our results emphasize the need to further investigate the connection between changes in the methylation of genes involved in myelination and phenotypes observed in WS individuals [21, 118, 122].

Other than myelination deficits, we identified abnormal methylation of the hypothalamic neuropeptide arginine vasopressin (AVP) in individuals with WS, which has been repeatedly implicated in mammalian social interactions and emotional states that support sociality [149–154]. AVP is involved in regulating the cardiovascular and autonomic systems, and in social behavior and adaptive functions [155, 156]. AVP is also involved in social cognition [152, 153, 157] and in the pathophysiology of many psychiatric conditions that include autism, depression, anxiety, borderline personality disorder and schizophrenia [152, 154]. Our results showing AVP hypomethylation converge with previous analysis of blood and brain [151, 158] samples from such individuals, which revealed exceptionally high AVP values, as compared to controls. These observations may provide further insight to the hyper-sociality of individuals with WS.

Overall, our findings suggest that the regulation of genes expression in WS is not affected solely by the haploinsufficiency of genes from the WSCR but also as a result of epigenetic modifications of genes involved in key pathways related to WS, such as myelination, brain development and social behavior and reinforce previous results shown by us and others.

It appears that aberrant methylations, as a result of the deletion of the WSCR locus, differently alters the epigenetic landscape of diverse cell types. Because we previously reported normal number of OLs in the brains of individuals with WS compared to TD controls [21], the altered methylation properties in OLs suggest intrinsic changes in DNA methylation in OLs in WS.

A few studies have suggested a possible correlation between the epigenetic landscape of the brain and peripheral tissue during disease progression, especially in cells of the blood [159, 160]. The identification of several putative targets may help with potentially earlier diagnosis in cases where limited resources and knowledge take place [161, 162], and perhaps more efficient treatment for individuals with WS. Nevertheless, the relatively low number of brain samples in our RRBS study, mainly due to the scarcity of WS in the population and specifically tissue donors with WS, may raise potential limitations. While we were able to improve our understanding of the genomic landscape of WS by identifying DMSs and DMRs significantly altered in individuals with WS compared to TD controls, further studies on the epigenome in WS using higher number of brain samples will be valuable in order to discover more insights on the DNA methylation changes associated with WS.

Evaluation of the human brain is extremely valuable for developing powerful diagnostic and therapeutic tools. Our results elucidated new genes involved in phenotypes observed in individuals with WS and the epigenetic profiles that lead to their dysregulation. These data further corroborate our earlier findings on myelin deficits in WS and offer new insight into additional genes involved in the process of proper myelination and neuronal function.

MATERIALS AND METHODS

Brain samples

All human tissue samples were kindly provided by the NIH NeuroBioBank at the University of Maryland, School of Medicine (NBB request #1068), in accordance with all legal provisions and relevant ethical considerations. Blocks of fresh-frozen control and WS human cortical brain samples from BA9 were examined.

DNA isolation, library preparation and sequencing

DNA was isolated using a QIAamp DNA micro-kit (#20-56304, Qiagen) according to the manufacturer’s instructions. Briefly, samples were incubated in lysis buffer containing proteinase K, heated and mixed in a thermomixer at 56°C overnight until completely lysed and then combined with buffer containing carrier RNA to increase the DNA yield. The samples were transferred through a QIAamp MinElute column for DNA binding, washed and eluted using an appropriate buffer. DNA concentrations were measured using a Nanodrop One apparatus (Thermo Fisher). RRBS libraries were prepared using a Zymo-Seq RRBS Library Kit (Zymo) at the Crown Genomics Institute of the Nancy and Stephen Grand Israel National Center for Personalized Medicine, Weizmann Institute of Science. Briefly, libraries were prepared from 100 ng of genomic DNA and quantified by Qubit (Thermo Fisher Scientific) and TapeStation (Agilent). Cytosine-to-Thymine (bisulfite) conversion efficiency was measured by aliquots of *Escherichia coli* genomic DNA, and determined as ~98%. Sequencing was performed on a NovaSeq 6000 instrument (Illumina) using an SP 100 cycle kit (single-end sequencing). An average of 54.2 million reads per sample was obtained.

Data analysis

Trimming of Illumina adapters, as well as quality trimming, was performed with Trim Galore, using the following options: --nextseq --non_directional --rrbs. Reads were mapped to the human genome (hg19) using Bismark v. 0.22-3, bowtie mode. We computed for each sample methylation proportion (*i.e.*, counting the number of methylated C’s versus number of unmethylated C’s) for each one of the identified CpG site (Bismark, methylation extractor mode, default setting). We then measured significant changes in methylation at each CpG site between individuals with WS and TD controls. Differential methylation of single CpG sites (DMSs) were extracted and calculated by edgeR generalized linear model (GLM) [76], with the recommended cutoff of at least 8 reads per sample. In addition, we included sex and age as covariates. The Benjamini-Hochberg multiple testing correction was applied to control for the false discovery rate (FDR < 0.05). DMRs were extracted and analyzed by metilene v. 0.2-8 [163]. For this analysis we used 300 bp as the maximum distance between CpGs to be allowed in the same segment, q-value cutoff of 0.01 and minimum average difference of 0.25. In addition, we performed paired analyses of DMRs, comparing (i) males to females (M vs. F), regardless of pathology; (ii) young vs. old (below and above the age median), regardless of pathology. These datasets were overlapped (via bedtools intersect) with the pathology comparison (TD vs. WS). Overlapped DMRs that could be skewed by these variables were excluded from the final list.

TF-binding motif enrichment analysis for DMSs were performed using HOMER [164] with a window of $-/+$ 25 bp around the CpG.

DMSs/DMRs in promoters, exons, 3’ and 5’ UTRs were annotated to genes using HOMER tools. In addition, DMSs/DMRs in introns and intergenic regions were mapped to their target genes by enhancer–promoter interactome data from Nott et al. 2019., where all cell types interactions were merged together.

Correlation analysis between differential DNA methylation and DEGs was performed by GeneOverlap R package [165]. Transcriptional data were taken from (i) brain samples from individuals with WS [21] or ASD [98], (ii) NPCs and neurons derived from WS fibroblasts [99] and (iii) brain samples from mice with *Gtf2i* deleted from excitatory neurons [21].

Table 1. Primers used for real-time qPCR (5'→3').

GENE	NCBI reference sequence	FWD	REV
<i>TUBA1B</i>	NC_000012.12	CGCCCGTCTCACTGAAGA	GCCAGATGCCAAGTGACAAG
<i>ID4</i>	NC_000006.12	CTGACTGCTGAACCCTACCTAA	TTTGAGGTTTACAGTCCACC
<i>GAD1</i>	NC_000002.12	CAAACCGTGCAATTCCTCCT	GCGATCAAATGTCTTGCGG
<i>LINGO3</i>	NC_000019.10	ATCCGCTGCTCAACCTC	GCAGCGTCTTAGCGTGT
<i>LINGO1</i>	NC_000015.10	AGCTTGAGAAGTCCCCTTG	TCTGACTTATCCAGCTCCTG
<i>GPR17</i>	NC_000002.12	CTGTTGCCTCTTCTACTC	GGATGAAAAGCCACAGAGC

Table 2. Primers used for 3C-qPCR (5'→3').

Enhancer	FWD	Promoter	REV
hypoDMS (<i>GPR17</i>)	GCATGGTGGGCCCTCATA	<i>GPR17</i>	CTGTGGTCTCCCTTCTCTC
control site (<i>GPR17</i>)	TGGGAGGTTCTGAAGGCATT	<i>GPR17</i>	CTGTGGTCTCCCTTCTCTC
hyperDMS (<i>LINGO1</i>)	GAGGAGGAGAAGTGGGTCCAG	<i>LINGO1</i>	CACTAGGAGCGAGCCAGG
control site (<i>LINGO1</i>)	TAGGAGCGAGCCAGGGAG	<i>LINGO1</i>	CACTAGGAGCGAGCCAGG

ChIP-seq data generated in the NIH roadmap epigenomics mapping consortium [97] were used to obtain genome-wide maps of H3K4me1 (GSM773014), H3K27ac (GSM1112810) and H3K9ac (GSM670021) profiles in the adult mid frontal region (Brodmann area 9/46). H3K4me1 and H3K27ac were overlapped with DMS/DMR location, via bedtools intersect. H3K9ac peaks were used to identify promoters sites and accordingly, to design primers for the 3C-qPCR assay.

For the cell-type specific analysis we used the enhancer or promoter locations, provided by the original study of Nott et al. 2019. GO analysis was performed using Metascape [166]. Integrative Genomics Viewer (IGV) tools were used for visualization [167].

RNA isolation, cDNA preparation and real-time polymerase chain reaction

RNA from BA9 cortex was isolated according to Kumar et al. (2021) [168] with minor modifications, briefly: 650 mg of fixed tissue was lysed in 400 µl TES buffer (500 mM Tris pH8, 100 mM EDTA, 100 mM NaCl, 1%SDS, 500 µg/ml proteinase K) and decossed in 56 °C for 3 hours. RNA was isolated from the lysates using TRI Reagent (Molecular Research Center) according to the manufacturer's instructions. RNA was reverse-transcribed to single-stranded cDNA by Super Script II Reverse Transcriptase (Thermo Fisher Scientific) and random primers were mixed with 1 µM gene specific primers (GSP) using a mix of reverse primers from the quantified genes; qPCR was performed in a CFX Connect Real-Time PCR Detection System (Bio-Rad) with PerfeCTa SYBR Green FastMix (Quanta BioSciences). Dissociation curves were analyzed following each real-time qPCR to confirm the presence of only one product and the absence of primer dimer formation. The threshold cycle number (Ct) for each tested gene (X) was used to quantify the relative abundance of that gene using the formula $2^{-(Ct_{geneX} - Ct_{standard})}$. Tubulin (*TUBA1B*) was used as the standard for mRNA expression. Primers used for the real-time qPCR and gene specific amplification are listed in Table 1.

Chromosome conformation capture (3C)-qPCR

3C was performed as previously described [169, 170] with minor modifications: fixation using 2% paraformaldehyde (Sigma) for 10 min, followed by lysis in a nuclear buffer: 0.5% Triton X-100 (Sigma), 0.1 M sucrose (Sigma), 5 Mm MgCl (Sigma), 1 mM EDTA (Sigma), 10 mM Tris pH 8 (Sigma). After resting on ice for 20 min, samples were digested using DpnII (New England Bio Labs) for 24 h at 37 °C with shaking at 1400 rpm, followed by inactivation for 20 min at 65 °C. Next, samples were cooled on ice and ligated with T4 DNA ligase (Invitrogen) for 22 h at 4 °C with shaking at 300 rpm. After ligation, samples were decossed with proteinase K (Invitrogen) overnight at 65 °C. DNA was extracted from the samples with DNA-purification buffers and spin columns (Cell Signaling Technology). Interaction frequencies were measured by qPCR with forward primers targeted to the promoter of *GPR17* and *LINGO1* and reverse primers targeting methylation sites.

Control primers were also designed to assess basal interaction levels of the promoter with non-specific loci, at the same genomic distance from

promoter as the methylation sites. The threshold cycle number (Ct) for each tested interaction (methylation site X) was used to quantify the relative frequency of that interaction. To validate specific interaction, the products of the qPCR were loaded onto a 2% agarose gel (Hydra gene) to verify a single band at expected product length. Samples presenting a smear or several nonspecific products were removed from the data. Primers used for the 3C-qPCR are listed in Table 2.

REFERENCES

- Morris CA. Introduction: Williams syndrome. *Am J Med Genet Part C: Semin Med Genet.* 2010;154C:203–8.
- Pober BR. Williams–Beuren Syndrome. *N. Engl J Med.* 2010;362:239–52.
- Kozel BA, Barak B, Kim CA, Mervis CB, Osborne LR, Porter M, et al. Williams syndrome. *Nat Rev Dis Primers.* 2021;7:42.
- Barak B, Feng G. Neurobiology of social behavior abnormalities in autism and Williams syndrome. *Nat Neurosci.* 2016;19:647–55.
- Zanella M, Vitriolo A, Andirko A, Martins PT, Sturm S, O'Rourke T, et al. Dosage analysis of the 7q11.23 Williams region identifies BAZ1B as a major human gene patterning the modern human face and underlying self-domestication. *Sci Adv.* 2019;5:eaaw7908.
- Cha SG, Song MK, Lee SY, Kim GB, Kwak JG, Kim WH, et al. Long-term cardiovascular outcome of Williams syndrome. *Congenit Heart Dis.* 2019;14:684–90.
- Del Pasqua A, Rinelli G, Toscano A, Iacobelli R, Digilio C, Marino B, et al. New findings concerning cardiovascular manifestations emerging from long-term follow-up of 150 patients with the Williams-Beuren-Beuren syndrome. *Cardiol Young.* 2009;19:563–7.
- Collins RT II. Cardiovascular disease in Williams syndrome. *Curr Opin Pediatr.* 2018;30:609–15.
- Pober BR, Wang E, Caprio S, Petersen KF, Brandt C, Stanley T, et al. High prevalence of diabetes and pre-diabetes in adults with Williams syndrome. *Am J Med Genet Part C: Semin Med Genet.* 2010;154C:291–8.
- Andersson SA, Olsson AH, Esguerra JLS, Heimann E, Ladenvall C, Edlund A, et al. Reduced insulin secretion correlates with decreased expression of exocytotic genes in pancreatic islets from patients with type 2 diabetes. *Mol Cell Endocrinol.* 2012;364:36–45.
- Frangiskakis JM, Ewart AK, Morris CA, Mervis CB, Bertrand J, Robinson BF, et al. LIM-kinase1 Hemizygoty Implicated in Impaired Visuospatial Constructive Cognition. *Cell.* 1996;86:59–69.
- Greiner de Magalhães C, Pitts CH, Mervis CB. Executive function as measured by the Behavior Rating Inventory of Executive Function-2: children and adolescents with Williams syndrome. *J Intellect Disabil Res.* 2022;66:94–107.
- Mervis CB, John AE. Cognitive and behavioral characteristics of children with Williams syndrome: Implications for intervention approaches. *Am J Med Genet Part C: Semin Med Genet.* 2010;154C:229–48.
- Miezah D, Porter M, Rossi A, Kazzi C, Batchelor J, Reeve J. Cognitive profile of young children with Williams syndrome. *J Intellect Disabil Res.* 2021;65:784–94.
- Meyer-Lindenberg A, Mervis CB, Faith Berman K. Neural mechanisms in Williams syndrome: a unique window to genetic influences on cognition and behaviour. *Nat Rev Neurosci.* 2006;7:380–93.

16. Morris CA, Braddock SR, Council On G, Chen E, Trotter TL, Berry SA, et al. Health care supervision for children with Williams Syndrome. *Pediatrics*. 2020;145:2019–3761.
17. Martens MA, Wilson SJ, Reutens DC. Research Review: Williams syndrome: a critical review of the cognitive, behavioral, and neuroanatomical phenotype. *J Child Psychol Psychiatry*. 2008;49:576–608.
18. Sanders Stephan J, Ercan-Sencicek AG, Hus V, Luo R, Murtha Michael T, Moreno-De-Luca D, et al. Multiple recurrent De Novo CNVs, Including duplications of the 7q11.23 Williams Syndrome Region, are strongly associated with Autism. *Neuron*. 2011;70:863–85.
19. Crespi BJ, Procyshyn TL. Williams syndrome deletions and duplications: Genetic windows to understanding anxiety, sociality, autism, and schizophrenia. *Neurosci Biobehav Rev*. 2017;79:14–26.
20. Mulle JG, Pulver AE, McGrath JA, Wolyniec PS, Dodd AF, Cutler DJ, et al. Reciprocal duplication of the Williams-Beuren Syndrome deletion on chromosome 7q11.23 is associated with Schizophrenia. *Biol Psychiatry*. 2014;75:371–7.
21. Barak B, Zhang Z, Liu Y, Nir A, Trangle SS, Ennis M, et al. Neuronal deletion of Gtf2i, associated with Williams syndrome, causes behavioral and myelin alterations rescuable by a remyelinating drug. *Nat Neurosci*. 2019;22:700–8.
22. Strong E, Butcher DT, Singhania R, Mervis CB, Morris CA, Carvalho DD, et al. Symmetrical dose-dependent DNA-methylation profiles in children with deletion or duplication of 7q11.23. *Am J Hum Genet*. 2015;97:216–27.
23. Kimura R, Lardenoije R, Tomiwa K, Funabiki Y, Nakata M, Suzuki S, et al. Integrated DNA methylation analysis reveals a potential role for ANKRD30B in Williams syndrome. *Neuropsychopharmacology*. 2020;45:1627–36.
24. Nir A, Barak B. White matter alterations in Williams syndrome related to behavioral and motor impairments. *Glia*. 2021;69:5–19.
25. Grad M, Nir A, Levy G, Trangle SS, Shapira G, Shomron N, et al. Altered white matter and microRNA expression in a murine model related to Williams Syndrome suggests that miR-34b/c affects brain development via Ptpu and Dcx Modulation. *Cells*. 2022;11:158.
26. Berger SL, Kouzarides T, Shiekhattar R, Shilatifard A. An operational definition of epigenetics. *Genes Dev*. 2009;23:781–3.
27. Bird A. Perceptions of epigenetics. *Nature*. 2007;447:396–8.
28. Nott A, Holtman IR, Coufal NG, Schlachetki JCM, Yu M, Hu R, et al. Brain cell type-specific enhancer-promoter interactome maps and disease-risk association. *Science*. 2019;366:1134.
29. Tsankova N, Renthal W, Kumar A, Nestler EJ. Epigenetic regulation in psychiatric disorders. *Nat Rev Neurosci*. 2007;8:355–67.
30. Cho KS, Elizondo LI, Boerkoel CF. Advances in chromatin remodeling and human disease. *Curr Opin Genet Dev*. 2004;14:308–15.
31. Kadach C, Crabtree GR. Mammalian SWI/SNF chromatin remodeling complexes and cancer: Mechanistic insights gained from human genomics. *Sci Adv*. 2015;1:e1500447.
32. Culver-Cochran AE, Chadwick BP. Loss of WSTF results in spontaneous fluctuations of heterochromatin formation and resolution, combined with substantial changes to gene expression. *BMC Genomics*. 2013;14:740.
33. Jangani M, Poolman TM, Matthews L, Yang N, Farrow SN, Berry A, et al. The Methyltransferase WBSR22/Merm1 enhances glucocorticoid receptor function and is regulated in lung inflammation and cancer. *J Biol Chem*. 2014;289:8931–46.
34. Schosserer M, Minois N, Angerer TB, Amring M, Dellago H, Harreither E, et al. Methylation of ribosomal RNA by NSUN5 is a conserved mechanism modulating organismal lifespan. *Nat Commun*. 2015;6:6158.
35. Peña-Hernández R, Marques M, Hilmi K, Zhao T, Saad A, Alaoui-Jamali MA, et al. Genome-wide targeting of the epigenetic regulatory protein CTCF to gene promoters by the transcription factor TFII-I. *Proc Natl Acad Sci USA*. 2015;112:E677–86.
36. Lazebnik MB, Tussie-Luna MI, Roy AL. Determination and functional analysis of the consensus binding site for TFII-I family member BEN, implicated in Williams-Beuren syndrome. *J Biol Chem*. 2008;283:11078–82.
37. Makeyev AV, Bayarsaihan D. ChIP-Chip Identifies SEC23A, CFDP1, and NSD1 as TFII-I Target Genes in Human Neural Crest Progenitor Cells. *Cleft Palate Craniofac J*. 2013;50:347–50.
38. Bayarsaihan D, Makeyev AV, Enkhmandakh B. Epigenetic modulation by TFII-I during embryonic stem cell differentiation. *J Cell Biochem*. 2012;113:3056–60.
39. Bayarsaihan D. What role does TFII-I have to play in epigenetic modulation during embryogenesis? *Epigenomics*. 2013;5:9–11.
40. Roy AL. Role of the multifunctional transcription factor TFII-I in DNA damage repair. *DNA Repair*. 2021;106:103175.
41. Makeyev AV, Enkhmandakh B, Hong SH, Joshi P, Shin DG, Bayarsaihan D. Diversity and complexity in chromatin recognition by TFII-I transcription factors in pluripotent embryonic stem cells and embryonic tissues. *PLoS One*. 2012;7:e44443.
42. Tussie-Luna MI, Bayarsaihan D, Seto E, Ruddle FH, Roy AL. Physical and functional interactions of histone deacetylase 3 with TFII-I family proteins and PIASxβ. *Proc Natl Acad Sci*. 2002;99:12807–12.
43. Crusselle-Davis VJ, Zhou Z, Anantharaman A, Moghimi B, Dodev T, Huang S, et al. Recruitment of coregulator complexes to the β-globin gene locus by TFII-I and upstream stimulatory factor. *FEBS J*. 2007;274:6065–73.
44. Hakimi M-A, Dong Y, Lane WS, Speicher DW, Shiekhattar R. A candidate X-linked mental retardation gene is a component of a new family of Histone Deacetylase-containing complexes. *J Biol Chem*. 2003;278:7234–9.
45. Pacaud R, Sery Q, Oliver L, Vallette FM, Tost J, Cartron P-F. DNMT3L interacts with transcription factors to target DNMT3L/DNMT3B to specific DNA sequences: Role of the DNMT3L/DNMT3B/p65-NfκB complex in the (de-)methylation of TRAF1. *Biochimie*. 2014;104:36–49.
46. Greenberg MVC, Bourc'his D. The diverse roles of DNA methylation in mammalian development and disease. *Nat Rev Mol Cell Biol*. 2019;20:590–607.
47. Yao B, Christian KM, He C, Jin P, Ming G-I, Song H. Epigenetic mechanisms in neurogenesis. *Nat Rev Neurosci*. 2016;17:537–49.
48. Guo H, Zhu P, Yan L, Li R, Hu B, Lian Y, et al. The DNA methylation landscape of human early embryos. *Nature*. 2014;511:606–10.
49. Smith ZD, Meissner A. DNA methylation: roles in mammalian development. *Nat Rev Genet*. 2013;14:204–20.
50. Moyon S, Huynh JL, Dutta D, Zhang F, Ma D, Yoo S, et al. Functional characterization of DNA methylation in the oligodendrocyte lineage. *Cell Rep*. 2016;15:748–60.
51. Liu J, Casaccia P. Epigenetic regulation of oligodendrocyte identity. *Trends Neurosci*. 2010;33:193–201.
52. Liu J, Moyon S, Hernandez M, Casaccia P. Epigenetic control of oligodendrocyte development: adding new players to old keepers. *Curr Opin Neurobiol*. 2016;39:133–8.
53. Aref-Eshghi E, Rodenhiser DJ, Schenkel LC, Lin H, Skinner C, Ainsworth P, et al. Genomic DNA methylation signatures enable concurrent diagnosis and clinical genetic variant classification in neurodevelopmental syndromes. *Am J Hum Genet*. 2018;102:156–74.
54. Corley MJ, Vargas-Maya N, Pang APS, Lum-Jones A, Li D, Khadka V, et al. Epigenetic delay in the neurodevelopmental trajectory of DNA methylation states in autism spectrum disorders. *Front Genet*. 2019;10:907.
55. Godler DE, Amor DJ. DNA methylation analysis for screening and diagnostic testing in neurodevelopmental disorders. *Essays Biochem*. 2019;63:785–95.
56. Moyon S, Ma D, Huynh JL, Coutts DJC, Zhao C, Casaccia P, et al. Efficient remyelination requires DNA methylation. *eNeuro*. 2017;4:ENEURO.0336-16.2017.
57. Moyon S, Casaccia P. DNA methylation in oligodendroglial cells during developmental myelination and in disease. *Neurogenesis* (Austin). 2017;4:e1270381.
58. Liu J, Magri L, Zhang F, Marsh NO, Albrecht S, Huynh JL, et al. Chromatin landscape defined by repressive histone methylation during oligodendrocyte differentiation. *J Neurosci*. 2015;35:352–65.
59. Huynh JL, Casaccia P. Defining the chromatin landscape in demyelinating disorders. *Neurobiol Dis*. 2010;39:47–52.
60. Liu J, Sandoval J, Doh ST, Cai L, López-Rodas G, Casaccia P. Epigenetic modifiers are necessary but not sufficient for reprogramming non-myelinating cells into myelin gene-expressing cells. *PLoS One*. 2010;5:e13023.
61. Jang HS, Shin WJ, Lee JE, Do JT. CpG and non-CpG methylation in epigenetic gene regulation and brain function. *Genes*. 2017;8:148.
62. Wang Z, Tang B, He Y, Jin P. DNA methylation dynamics in neurogenesis. *Epigenomics*. 2016;8:401–14.
63. Sandoval J, Heyn H, Moran S, Serra-Musach J, Pujana MA, Bibikova M, et al. Validation of a DNA methylation microarray for 450,000 CpG sites in the human genome. *Epigenetics*. 2011;6:692–702.
64. Ladd-Acosta C, Hansen KD, Briem E, Fallin MD, Kaufmann WE, Feinberg AP. Common DNA methylation alterations in multiple brain regions in autism. *Mol Psychiatry*. 2014;19:862–71.
65. Numata S, Ye T, Herman M, Lipska BK. DNA methylation changes in the post-mortem dorsolateral prefrontal cortex of patients with schizophrenia. *Front Genet*. 2014;5:280.
66. Veyrac A, Besnard A, Caboche J, Davis S, Laroche S. Chapter Four - The Transcription Factor Zif268/Egr1, Brain Plasticity, and Memory, in *Progress in Molecular Biology and Translational Science*, ZU Khan and EC Muly, Editors. 2014, Academic Press. 89–129.
67. O'Donovan KJ, Tourtellotte WG, Millbrandt J, Baraban JM. The EGR family of transcription-regulatory factors: progress at the interface of molecular and systems neuroscience. *Trends Neurosci*. 1999;22:167–73.
68. Bacon C, Rappold GA. The distinct and overlapping phenotypic spectra of FOXP1 and FOXP2 in cognitive disorders. *Hum Genet*. 2012;131:1687–98.

69. Lee B-K, Iyer VR. Genome-wide studies of CCCTC-binding Factor (CTCF) and cohesin provide insight into chromatin structure and regulation. *J Biol Chem*. 2012;287:30906–13.
70. Semick SA, Bharadwaj RA, Collado-Torres L, Tao R, Shin JH, Deep-Soboslay A, et al. Integrated DNA methylation and gene expression profiling across multiple brain regions implicate novel genes in Alzheimer's disease. *Acta Neuropathol*. 2019;137:557–69.
71. Marin-Husstege M, He Y, Li J, Kondo T, Sablitzky F, Casaccia-Bonneli P. Multiple roles of Id4 in developmental myelination: Predicted outcomes and unexpected findings. *Glia*. 2006;54:285–96.
72. Kondo T, Raff M. The Id4 HLH protein and the timing of oligodendrocyte differentiation. *EMBO J*. 2000;19:1998–2007.
73. Guillemain A, Laouarem Y, Cobret L, Štefok D, Chen W, Bloch S, et al. LINGO family receptors are differentially expressed in the mouse brain and form native multimeric complexes. *FASEB J*. 2020;34:13641–53.
74. Mi S, Hu B, Hahm K, Luo Y, Kam Hui ES, Yuan Q, et al. LINGO-1 antagonist promotes spinal cord remyelination and axonal integrity in MOG-induced experimental autoimmune encephalomyelitis. *Nat Med*. 2007;13:1228–33.
75. Mi S, Miller RH, Lee X, Scott ML, Shulag-Morskaya S, Shao Z, et al. LINGO-1 negatively regulates myelination by oligodendrocytes. *Nat Neurosci*. 2005;8:745–51.
76. Chen Y, Pal B, Visvader JE, Smyth GK. Differential methylation analysis of reduced representation bisulfite sequencing experiments using edgeR. *F1000Research*. 2017;6:2055.
77. Maunakea AK, Nagarajan RP, Bilenyk M, Ballinger TJ, D'Souza C, Fouse SD, et al. Conserved role of intragenic DNA methylation in regulating alternative promoters. *Nature*. 2010;466:253–7.
78. Spindola LM, Santoro ML, Pan PM, Ota VK, Xavier G, Carvalho CM, et al. Detecting multiple differentially methylated CpG sites and regions related to dimensional psychopathology in youths. *Clin Epigenetics*. 2019;11:146.
79. Jeong H, Mendizabal I, Berto S, Chatterjee P, Layman T, Usui N, et al. Evolution of DNA methylation in the human brain. *Nat Commun*. 2021;12:2021.
80. Heinz S, Benner C, Spann N, Bertolino E, Lin YC, Laslo P, et al. Simple combinations of lineage-determining transcription factors prime cis-regulatory elements required for macrophage and B cell identities. *Mol Cell*. 2010;38:576–89.
81. Roth RB, Hevezi P, Lee J, Willhite D, Lechner SM, Foster AC, et al. Gene expression analyses reveal molecular relationships among 20 regions of the human CNS. *Neurogenetics*. 2006;7:67–80.
82. Lin A, Wang RT, Ahn S, Park CC, Smith DJ. A genome-wide map of human genetic interactions inferred from radiation hybrid genotypes. *Genome Res*. 2010;20:1122–32.
83. Beckmann AM, Wilce PA. Egr transcription factors in the nervous system. *Neurochemistry Int*. 1997;31:477–510.
84. Kim SH, Song JY, Joo EJ, Lee KY, Shin SY, Lee YH, et al. Genetic association of the EGR2 gene with bipolar disorder in Korea. *Exp Mol Med*. 2012;44:121–9.
85. Morris ME, Viswanathan N, Kuhlman S, Davis FC, Weitz CJ. A screen for genes induced in the suprachiasmatic nucleus by light. *Science*. 1998;279:1544–7.
86. Hu VW, Frank BC, Heine S, Lee NH, Quackenbush J. Gene expression profiling of lymphoblastoid cell lines from monozygotic twins discordant in severity of autism reveals differential regulation of neurologically relevant genes. *BMC Genomics*. 2006;7:118.
87. Wang T, Xiong J-Q. The orphan nuclear receptor TLX/NR2E1 in neural stem cells and diseases. *Neurosci Bull*. 2016;32:108–14.
88. Zhang C-L, Zou Y, He W, Gage FH, Evans RM. A role for adult TLX-positive neural stem cells in learning and behaviour. *Nature*. 2008;451:1004–7.
89. Kumar RA, McGhee KA, Leach S, Bonaguro R, Maclean A, Aguirre-Hernandez R, et al. Initial association of NR2E1 with bipolar disorder and identification of candidate mutations in bipolar disorder, schizophrenia, and aggression through resequencing. *Am J Med Genet Part B: Neuropsychiatr Genet*. 2008;147B:880–9.
90. O'Leary JD, Kozareva DA, Hueston CM, O'Leary OF, Cryan JF, Nolan YM. The nuclear receptor Tlx regulates motor, cognitive and anxiety-related behaviours during adolescence and adulthood. *Behav Brain Res*. 2016;306:36–47.
91. Yamakawa H, Cheng J, Penney J, Gao F, Rueda R, Wang J, et al. The Transcription Factor Sp3 cooperates with HDAC2 to regulate synaptic function and plasticity in neurons. *Cell Rep*. 2017;20:1319–34.
92. Thumfart KM, Jawaid A, Bright K, Flachsman M, Mansuy IM. Epigenetics of childhood trauma: Long term sequelae and potential for treatment. *Neurosci Biobehav Rev*. 2022;132:1049–66.
93. Day JJ, Kennedy AJ, Sweatt JD. DNA Methylation and its implications and accessibility for neuropsychiatric therapeutics. *Annu Rev Pharmacol Toxicol*. 2015;55:591–611.
94. Meaney MJ, Szyf M. Environmental programming of stress responses through DNA methylation: life at the interface between a dynamic environment and a fixed genome. *Dialogues Clin Neurosci*. 2005;7:103–23.
95. Rajarajan P, Gil SE, Brennand KJ, Akbarian S. Spatial genome organization and cognition. *Nat Rev Neurosci*. 2016;17:681–91.
96. Kempfer R, Pombo A. Methods for mapping 3D chromosome architecture. *Nat Rev Genet*. 2020;21:207–26.
97. Bernstein BE, Stamatoyannopoulos Ja, Costello Jf, Ren B, Milosavljevic A, Meissner A, et al. The NIH Roadmap Epigenomics Mapping Consortium. *Nat Biotechnol*. 2010;28:1045–8.
98. Irimia M, Weatheritt RJ, Ellis JD, Parikhshak NN, Gonatopoulos-Pournatzis T, Babor M, et al. A highly conserved program of neuronal microexons is misregulated in autistic brains. *Cell*. 2014;159:1511–23.
99. Chailangkarn T, Trujillo CA, Freitas BC, Hrvoj-Mihic B, Herai RH, Yu DX, et al. A human neurodevelopmental model for Williams syndrome. *Nature*. 2016;536:338–43.
100. Zhou J, Sears RL, Xing X, Zhang B, Li D, Rockweiler NB, et al. Tissue-specific DNA methylation is conserved across human, mouse, and rat, and driven by primary sequence conservation. *BMC Genomics*. 2017;18:724.
101. Lökk K, Modhukur V, Rajashekar B, Märtens K, Mägi R, Kolde R, et al. DNA methylome profiling of human tissues identifies global and tissue-specific methylation patterns. *Genome Biol*. 2014;15:3248.
102. Andrews SV, Ellis SE, Bakulski KM, Sheppard B, Croen LA, Hertz-Picciotto I, et al. Cross-tissue integration of genetic and epigenetic data offers insight into autism spectrum disorder. *Nat Commun*. 2017;8:1011.
103. Pott S, Lieb JD. What are super-enhancers? *Nat Genet*. 2015;47:8–12.
104. Simons M, Trajkovic K. Neuron-glia communication in the control of oligodendrocyte function and myelin biogenesis. *J Cell Sci*. 2006;119:4381–9.
105. Barres BA, Schmid R, Sendtner M, Raff MC. Multiple extracellular signals are required for long-term oligodendrocyte survival. *Development*. 1993;118:283–95.
106. Fields RD, Stevens-Graham B. New insights into neuron-glia communication. *Science*. 2002;298:556–62.
107. Mitew S, Hay CM, Peckham H, Xiao J, Koenning M, Emery B. Mechanisms regulating the development of oligodendrocytes and central nervous system myelin. *Neuroscience*. 2014;276:29–47.
108. Bilican B, Fiore-Herliche C, Compston A, Allen ND, Chandran S. Induction of Olig2+ precursors by FGF involves BMP signalling blockade at the smad level. *PLOS ONE*. 2008;3:e2863.
109. Michailov Galin V, Sereda Michael V, Brinkmann Bastian G, Fischer Tobias M, Haug B, Birchmeier C, et al. Axonal Neuregulin-1 regulates myelin sheath thickness. *Science*. 2004;304:700–3.
110. Xiao J, Ferner AH, Wong AW, Denham M, Kilpatrick TJ, Murray SS. Extracellular signal-regulated kinase 1/2 signaling promotes oligodendrocyte myelination in vitro. *J Neurochemistry*. 2012;122:1167–80.
111. Xiao J, Wong AW, Willingham MM, van den Buuse M, Kilpatrick TJ, Murray SS. Brain-derived neurotrophic factor promotes central nervous system myelination via a direct effect upon oligodendrocytes. *Neurosignals*. 2010;18:186–202.
112. Gendron-Maguire M, Mallo M, Zhang M, Gridley T. Hoxa-2 mutant mice exhibit homeotic transformation of skeletal elements derived from cranial neural crest. *Cell*. 1993;75:1317–31.
113. Santagati F, Minoux M, Ren S-Y, Rijli FM. Temporal requirement of Hoxa2 in cranial neural crest skeletal morphogenesis. *Development*. 2005;132:4927–36.
114. Tavella S, Bobola N. Expressing Hoxa2 across the entire endochondral skeleton alters the shape of the skeletal template in a spatially restricted fashion. *Differentiation*. 2010;79:194–202.
115. Boeckx, C and Benítez-Burraco A, Osteogenesis and neurogenesis: a robust link also for language evolution. *Front Cell Neurosci*, 2015. 9.
116. Fukushima N, Furuta D, Hidaka Y, Moriyama R, Tsujiuchi T. Post-translational modifications of tubulin in the nervous system. *J Neurochemistry*. 2009;109:683–93.
117. Gadadhar S, Alvarez Viar G, Hansen JN, Gong A, Kostarev A, laly-Radio C, et al. Tubulin glycylation controls axonemal dynein activity, flagellar beat, and male fertility. *Science*. 2021;371:6525.
118. Jang S-W, Srinivasan R, Jones EA, Sun G, Keles S, Krueger C, et al. Locus-wide identification of Egr2/Krox20 regulatory targets in myelin genes. *J Neurochemistry*. 2010;115:1409–20.
119. Kuhlbrodt K, Herbarth B, Sock E, Hermans-Borgmeyer I, Wegner M. Sox10, a novel transcriptional modulator in glial cells. *J Neurosci*. 1998;18:237.
120. LeBlanc SE, Jang S-W, Ward RM, Wrabetz L, Svaren J. Direct regulation of myelin protein zero expression by the Egr2 transactivator. *J Biol Chem*. 2006;281:5453–60.
121. Swanberg SE, Nagarajan RP, Peddada S, Yasui DH, LaSalle JM. Reciprocal co-regulation of EGR2 and MECP2 is disrupted in Rett syndrome and autism. *Hum Mol Genet*. 2009;18:525–34.
122. Mager GM, Ward RM, Srinivasan R, Jang S-W, Wrabetz L, Svaren J. Active gene repression by the Egr2-NAB complex during peripheral nerve myelination. *J Biol Chem*. 2008;283:18187–97.

123. Le N, Nagarajan R, Wang JYT, Svaren J, LaPash C, Araki T, et al. Nab proteins are essential for peripheral nervous system myelination. *Nat Neurosci*. 2005;8:932–40.
124. Okano M, Bell DW, Haber DA, Li E. DNA Methyltransferases Dnmt3a and Dnmt3b are essential for De Novo methylation and mammalian development. *Cell*. 1999;99:247–57.
125. Gertz J, Varley KE, Reddy TE, Bowling KM, Pauli F, Parker SL, et al. Analysis of DNA methylation in a three-generation family reveals widespread genetic influence on epigenetic regulation. *PLOS Genet*. 2011;7:e1002228.
126. Gölzenleuchter M, Kanwar R, Zaibak M, Al Saiegh F, Hartung T, Klukas J, et al. Plasticity of DNA methylation in a nerve injury model of pain. *Epigenetics*. 2015;10:200–12.
127. Nohara K, Nakabayashi K, Okamura K, Suzuki T, Suzuki S, Hata K. Gestational arsenic exposure induces site-specific DNA hypomethylation in active retrotransposon subfamilies in offspring sperm in mice. *Epigenetics Chromatin*. 2020;13:53.
128. Voisin A-S, Suarez Ulloa V, Stockwell P, Chatterjee A, Silvestre F, Genome-wide DNA methylation of the liver reveals delayed effects of early-life exposure to 17 α -ethinylestradiol in the self-fertilizing mangrove rivulus. *Epigenetics*. 2022;17:473–97.
129. Baker Frost D, da Silveira W, Hazard ES, Atanelishvili I, Wilson RC, Flume J, et al. Differential DNA methylation landscape in skin fibroblasts from African Americans with systemic Sclerosis. *Genes*. 2021;12:129.
130. Raff MC, Miller RH, Noble M. A glial progenitor cell that develops in vitro into an astrocyte or an oligodendrocyte depending on culture medium. *Nature*. 1983;303:390–6.
131. Raff MC, Abney ER, Fok-Seang J. Reconstitution of a developmental clock in vitro: a critical role for astrocytes in the timing of oligodendrocyte differentiation. *Cell*. 1985;42:61–9.
132. Raff MC, Lillien LE, Richardson WD, Burne JF, Noble MD. Platelet-derived growth factor from astrocytes drives the clock that times oligodendrocyte development in culture. *Nature*. 1988;333:562–5.
133. Mi S, Lee X, Shao Z, Thill G, Ji B, Relton J, et al. LINGO-1 is a component of the Nogo-66 receptor/p75 signaling complex. *Nat Neurosci*. 2004;7:221–8.
134. Riechmann V, van Cruchten I, Sablitzky F. The expression pattern of Id4, a novel dominant negative helix-loop-helix protein, is distinct from Id1, Id2 and Id3. *Nucleic Acids Res*. 1994;22:749–55.
135. Jen Y, Manova K, Benezra R. Expression patterns of Id1, Id2, and Id3 are highly related but distinct from that of Id4 during mouse embryogenesis. *Dev Dyn: Off Publ Am Assoc Anatomists*. 1996;207:235–52.
136. Norton JD, Deed RW, Craggs G, Sablitzky F. Id helix—loop—helix proteins in cell growth and differentiation. *Trends Cell Biol*. 1998;8:58–65.
137. Norton JD, Atherton GT. Coupling of cell growth control and apoptosis functions of Id proteins. *Mol Cell Biol*. 1998;18:2371–81.
138. Emery B. Regulation of oligodendrocyte differentiation and myelination. *Science*. 2010;330:779–82.
139. Plemel JR, Manesh SB, Sparling JS, Tetzlaff W. Myelin inhibits oligodendroglial maturation and regulates oligodendrocytic transcription factor expression. *Glia*. 2013;61:1471–87.
140. Huang H-S, Akbarian S. GAD1 mRNA expression and DNA methylation in prefrontal cortex of subjects with Schizophrenia. *PLOS ONE*. 2007;2:e809.
141. Tao R, Davis KN, Li C, Shin JH, Gao Y, Jaffe AE, et al. GAD1 alternative transcripts and DNA methylation in human prefrontal cortex and hippocampus in brain development, schizophrenia. *Mol Psychiatry*. 2018;23:1496–505.
142. Yizhar O, Fenno LE, Prigge M, Schneider F, Davidson TJ, O'Shea DJ, et al. Neocortical excitation/inhibition balance in information processing and social dysfunction. *Nature*. 2011;477:171–8.
143. Levy DR, Tamir T, Kaufman M, Parabucki A, Weissbrod A, Schneidman E, et al. Dynamics of social representation in the mouse prefrontal cortex. *Nat Neurosci*. 2019;22:2013–22.
144. Yizhar O, Levy DR. The social dilemma: prefrontal control of mammalian sociability. *Curr Opin Neurobiol*. 2021;68:67–75.
145. Chew L-J, Coley W, Cheng Y, Gallo V. Mechanisms of regulation of oligodendrocyte development by p38 Mitogen-activated Protein Kinase. *J Neurosci*. 2010;30:11011–27.
146. Liang X, Draghi NA, Resh MD. Signaling from Integrins to Fyn to Rho Family GTPases regulates morphologic differentiation of Oligodendrocytes. *J Neurosci*. 2004;24:7140.
147. Chen Y, Wu H, Wang S, Koito H, Li J, Ye F, et al. The oligodendrocyte-specific G protein-coupled receptor GPR17 is a cell-intrinsic timer of myelination. *Nat Neurosci*. 2009;12:1398–406.
148. Boda E, Viganò F, Rosa P, Fumagalli M, Labat-Gest V, Tempia F, et al. The GPR17 receptor in NG2 expressing cells: Focus on in vivo cell maturation and participation in acute trauma and chronic damage. *Glia*. 2011;59:1958–73.
149. Carter CS, Grippo AJ, Pournajafi-Nazarloo H, Ruscio MG, and Porges SW. *Oxytocin, vasopressin and sociality*, in *Progress in Brain Research*, ID Neumann and R Landgraf, Editors. 2008, Elsevier. 331–6.
150. Heinrichs M, von Dawans B, Domes G. Oxytocin, vasopressin, and human social behavior. *Front Neuroendocrinol*. 2009;30:548–57.
151. Dai L, Carter CS, Ying J, Bellugi U, Pournajafi-Nazarloo H, Korenberg JR. Oxytocin and Vasopressin are dysregulated in Williams syndrome, a genetic disorder affecting social behavior. *PLOS ONE*. 2012;7:e38513.
152. Meyer-Lindenberg A, Domes G, Kirsch P, Heinrichs M. Oxytocin and vasopressin in the human brain: social neuropeptides for translational medicine. *Nat Rev Neurosci*. 2011;12:524–38.
153. Johnson ZV, Young LJ. Oxytocin and vasopressin neural networks: Implications for social behavioral diversity and translational neuroscience. *Neurosci Biobehav Rev*. 2017;76:87–98.
154. Ebstein RP, Knafo A, Mankuta D, Chew SH, Lai PS. The contributions of oxytocin and vasopressin pathway genes to human behavior. *Hormones Behav*. 2012;61:359–79.
155. Landgraf R, Neumann ID. Vasopressin and oxytocin release within the brain: a dynamic concept of multiple and variable modes of neuropeptide communication. *Front Neuroendocrinol*. 2004;25:150–76.
156. Sue Carter C. Neuroendocrine perspectives on social attachment and love. *Psychoneuroendocrinology*. 1998;23:779–818.
157. Insel TR. The challenge of translation in social neuroscience: a review of oxytocin, vasopressin, and affiliative behavior. *Neuron*. 2010;65:768–79.
158. Haas BW and Smith AK, Oxytocin, vasopressin, and Williams syndrome: epigenetic effects on abnormal social behavior. *Front Genet*, 2015. 6.
159. Bakulski KM, Halladay A, Hu VW, Mill J, Fallin MD. Epigenetic research in neuropsychiatric disorders: the “Tissue Issue”. *Curr Behav Neurosci Rep*. 2016;3:264–74.
160. Nestler EJ, Peña CJ, Kundakovic M, Mitchell A, Akbarian S. Epigenetic basis of mental illness. *Neuroscientist*. 2015;22:447–63.
161. Tekendo-Ngongang C, Dahoun S, Nguéfac S, Gimelli S, Sloan-Béna F, Wonkam A. Challenges in clinical diagnosis of Williams-beuren syndrome in sub-saharan africans: case reports from cameroon. *Mol Syndromol*. 2014;5:287–92.
162. Lumaka A, Lukoo R, Mubungu G, Lumbala P, Mbayabo G, Mupuala A, et al. Williams-Beuren syndrome: pitfalls for diagnosis in limited resources setting. *Clin Case Rep*. 2016;4:294–7.
163. Jühling F, Kretzmer H, Bernhart SH, Otto C, Stadler PF, Hoffmann S. metilene: fast and sensitive calling of differentially methylated regions from bisulfite sequencing data. *Genome Res*. 2016;26:256–62.
164. Heinz S, Benner C, Spann N, Bertolino E, Lin YC, Laslo P, et al. Simple combinations of lineage-determining transcription factors prime cis-regulatory elements required for macrophage and B cell identities. *Mol Cell*. 2010;38:576–89.
165. Shen L. Gene Overlap: Test and visualize gene overlaps. 0.99.0. 2013. <https://doi.org/10.18129/B9.bioc.GeneOverlap>.
166. Zhou Y, Zhou B, Pache L, Chang MA-OX, Khodabakhshi AH, Tanaseichuk O, et al. Metascape provides a biologist-oriented resource for the analysis of systems-level datasets. *Nat Commun*. 2019;10:1523.
167. Robinson JT, Thorvaldsdóttir H, Winckler W, Guttman M, Lander ES, Getz G, et al. Integrative genomics viewer. *Nat Biotechnol*. 2011;29:24–26.
168. Kumar K, Oli A, Hallikeri K, Shilpasree AS, Goni M. An optimized protocol for total RNA isolation from archived formalin-fixed paraffin-embedded tissues to identify the long non-coding RNA in oral squamous cell carcinomas. *MethodsX*. 2021;9:101602.
169. Oudelaar AM, Downes DJ, Davies JOJ, Hughes JR. Low-input Capture-C: A chromosome conformation capture assay to analyze chromatin architecture in small numbers of cells. *Bio Protoc*. 2017;7:e2645.
170. Splinter E, Grosveld F, de Laat W. 3C technology: analyzing the spatial organization of genomic loci in vivo. *Methods Enzymol*. 2004;375:493–507.

ACKNOWLEDGEMENTS

The authors acknowledge the input from the members of the Barak and Marco laboratories on the manuscript and the study. Human tissue was obtained from the NIH NeuroBioBank at the University of Maryland. We thank the donors of the brain tissue and their families for their invaluable donations for the advancement of scientific understanding. This work is supported by grants from the Fritz Thyssen Stiftung (Ref. 10.19.1.011MN) and the Israeli Science Foundation (Number 2305/20).

AUTHOR CONTRIBUTIONS

SST, AM, and BB designed the experiments and wrote the manuscript. SST, TR, HP, GL, EB, AM and BB collected, analyzed and interpreted the results.

COMPETING INTERESTS

The authors declare no competing interests.

ADDITIONAL INFORMATION

Supplementary information The online version contains supplementary material available at <https://doi.org/10.1038/s41380-022-01921-z>.

Correspondence and requests for materials should be addressed to Asaf Marco or Boaz Barak.

Reprints and permission information is available at <http://www.nature.com/reprints>

Publisher's note Springer Nature remains neutral with regard to jurisdictional claims in published maps and institutional affiliations.

Springer Nature or its licensor (e.g. a society or other partner) holds exclusive rights to this article under a publishing agreement with the author(s) or other rightsholder(s); author self-archiving of the accepted manuscript version of this article is solely governed by the terms of such publishing agreement and applicable law.